Check for updates

Wiley
Journal of Engineering
Volume 2026, Article ID 9725460, 43 pages
https://doi.org/10.1155/je/9725460

WILEY

Research Article

Dynamic Response of Spherically Curved Laminated Plate Subjected to Sudden Loading

Salih N. Akour and Zaid Abd Al-Hadi

Department of Mechanical Engineering, School of Engineering, The University of Jordan, Amman, Jordan

Correspondence should be addressed to Salih N. Akour; akour@ju.edu.jo

Received 11 August 2025; Revised 9 November 2025; Accepted 14 November 2025

Academic Editor: Bhimappa Suresha

Copyright © 2026 Salih N. Akour and Zaid Abd Al-Hadi. Journal of Engineering published by John Wiley & Sons Ltd. This is an open access article under the terms of the Creative Commons Attribution License, which permits use, distribution and reproduction in any medium, provided the original work is properly cited.

This study investigated the dynamic response of simply supported spherical laminated composite plates with square vertices, composed of graphite/epoxy material, under sudden loading. The research examined the influence of stacking sequence, thickness variation, and type of loading using the finite element method (FEM). The results demonstrated that stacking sequence significantly affects plate deformation, where the anti-symmetric laminates exhibited higher deformation compared to symmetric laminates. The unidirectional and cross-ply laminates displayed the least deformation. Furthermore, while the stacking sequence modulates the amplitude's response, it does not affect the frequency characteristics. Regardless of load type, laminates subjected to pressure or moment loading showed no change in the frequency characteristics. Thickness variation notably influences the amplitude characteristics but not the frequency characteristics, indicating the ability to control the amplitude modulation of the response by controlling these parameters.

1. Introduction

Composite materials are highly recognized for their remarkable mechanical properties and versatility. Composites offer unparalleled advantages such as exceptional strength-to-weight ratio, corrosion resistance, and design flexibility. Among numerous applications of composite materials, laminated composite plates stand out as fundamental structural element. They are widely used in critical sectors including aerospace, automotive, and marine. The dynamic response of composite plates under sudden loading scenarios is a subject of primary importance, thus necessitating comprehensive investigation to understand and mitigate potential challenges. Impact loading, characterized by sudden and transient forces applied to a structure, poses unique consideration for composite plate structures, including structural integrity, energy absorption, and response control and/or mitigation [1]. Research on curved composite plates demonstrates their complex mechanical behavior, which is highly dependent on their geometry and layer orientation. Studies show that the curvature significantly influences buckling resistance and free vibration characteristics, with specific layup sequences being crucial for optimizing structural stability. Furthermore, the dynamic response, including how these curved plates vibrate and respond to impacts, is distinctly different from flat panels, requiring specialized analytical and finite element models to accurately predict their performance and failure modes for advanced engineering applications.

Similar challenges are encountered in spacecraft design, particularly in solar panels mounted on large flexible appendages. These structures are frequently subjected to abrupt temperature changes in space, where one side of the appendages face direct solar radiation, while the other remain in shadow. Such temperature changes induce thermal stresses; these thermal stresses, combined with the dynamic forces from space operations, require a thorough understanding of the material's dynamic response to ensure the durability and reliability of the structure [2]. Composite materials can be tailored to achieve characteristics that are unique and mostly unattainable by any individual material. This versatility made composites to be utilized in a wide range of applications, especially the critical ones such as mentioned earlier. This triggered significant attention and

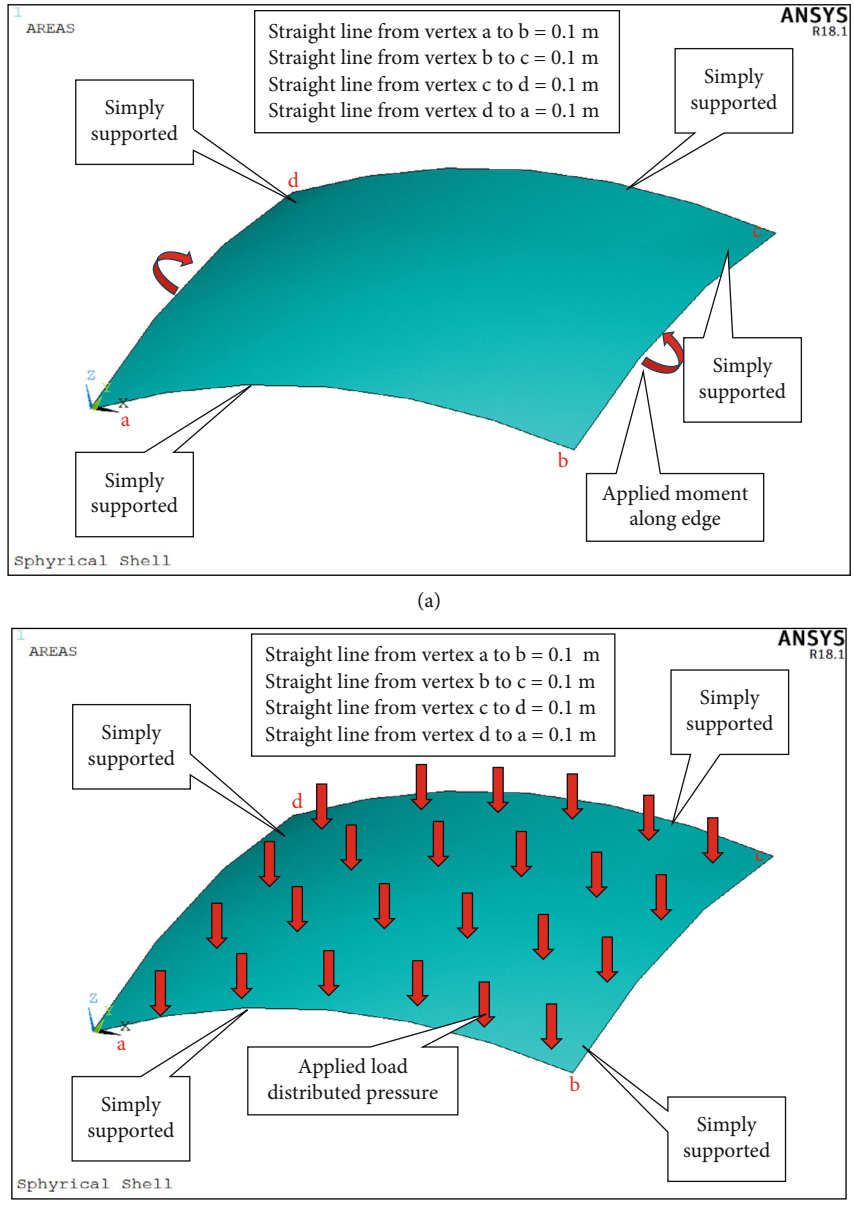


Figure 1: Model structure. (a) Model under moment load. (b) Model under pressure load.

interest among researchers. Mallikarjuna et al. developed a higher-order isoparametric finite element model to analyze the response of symmetric laminated composite plates by employing an explicit time-marching scheme. The results were compared to those obtained from Mindlin theory, where it demonstrated more accuracy in predicting displacement and stresses [3]. Kant et al. conducted a numerical convergence and stability study between three different finite elements (four-node linear, eight-node serendipity, and nine-node Lagrangian), to investigate the accuracy of these elements to model the transverse shear effects in multilayered sandwich panels based on Mindlin theory [4]. Kant et al. extended the research by considering composites plates, as well as studying the sandwich plates. The study utilized the same nine-noded Lagrangian element. However, the model is based on higher-order shear deformation theory, and the solution is employed using the superposition method. The solution technique provided good results as the direct numerical integration, but more efficient in computational time [5]. Carvalho et al. investigated the dynamic response of rectangular composite plates subjected to lateral loads by comparing a numerical formulation to an analytical solution. Both methods utilized Fourier expansion to solve the equation of motion. The study found good agreement between the analytical solution and the numerical solution in terms of contact forces and displacement. However, there was a notable discrepancy in peak strain values, which was not explained [6]. Chen et al. developed a semi-analytical finite strip method to analyze geometrically nonlinear response to dynamic loading of composite laminated plates.

3962, 2026, 1, Downloaded from https://onlinelibrary.wiley.com/doi/10.1155/je/9725460 by Turkey Cochrane Evidence Aid, Wiley Online Library on [01/10/2026]. See the Terms and Conditions (https://onlinelibrary.wiley.com/terms-and-conditions) on Wiley Online Library for rules of use; OA articles are governed by the applicable Creative Commons License

TABLE 1: Material properties of epoxy/carbon lamina [28, 29].

Material	Property	Value	Unit
Epoxy/graphite	Modulus of elasticity, E_x	3.089	GPa
	Modulus of elasticity, E_y	5.586	GPa
	Modulus of elasticity, E_z	5.586	GPa
	Shear modulus, G_{xy}	5.368	GPa
	Shear modulus, G_{xz}	5.368	GPa
	Shear modulus, G_{yz}	1.395	GPa
	Major Poisson's ratio, ν_{xy}	0.23252	
	Minor Poisson's ratio	0.4316	
	Density	1659	kg/m^3
Resin epoxy (Araldite LY1564)	Modulus of elasticity	3.78	GPa
	Poisson's ratio	0.35	
	Density	1200	kg/m^3
Fibers (PYROFIL HR40)	Modulus of elasticity	3.78	GPa
	Poisson's ratio	0.2	
	Density	1820	kg/m^3

TABLE 2: Stiffness matrices for each stacking sequence.

Laminate name	Stacking sequence	Stiffness
Unidirectional	[0, 0, 0, 0, 0]	$A_{11} \neq 0, A_{12} \neq 0, A_{22} \neq 0, A_{66} \neq 0, A_{16} = 0, A_{26} = 0$ $B_{ij} = 0$ $D_{11} \neq 0, D_{12} \neq 0, D_{22} \neq 0, D_{66} \neq 0, D_{16} = 0, D_{26} = 0$
Cross-ply	[0, 90, 0, 90, 0]	$A_{11} \neq 0, A_{12} \neq 0, A_{22} \neq 0, A_{66} \neq 0, A_{16} = 0, A_{26} = 0$ $B_{ij} = 0$ $D_{11} \neq 0, D_{12} \neq 0, D_{22} \neq 0, D_{66} \neq 0, D_{16} = 0, D_{26} = 0$
Symmetric-30	[30, − 30, 0, − 30, 30]	$A_{11} \neq 0, A_{12} \neq 0, A_{22} \neq 0, A_{66} \neq 0, A_{16} = 0, A_{26} = 0$ $B_{ij} = 0, D_{ij} \neq 0$
Symmetric-45	[45, − 45, 0, − 45, 45]	$A_{11} \neq 0, A_{12} \neq 0, A_{22} \neq 0, A_{66} \neq 0, A_{16} = 0, A_{26} = 0$ $B_{ij} = 0, D_{ij} \neq 0$
Anti-symmetric-30	[30, − 30, 0, 30, − 30]	$A_{11} \neq 0, A_{12} \neq 0, A_{22} \neq 0, A_{66} \neq 0, A_{16} = 0, A_{26} = 0$ $B_{11} = 0, B_{12} = 0, B_{22} = 0, B_{66} = 0, B_{16} \neq 0, B_{26} \neq 0$ $D_{11} \neq 0, D_{12} \neq 0, D_{22} \neq 0, D_{66} \neq 0, D_{16} = 0, D_{26} = 0$
Anti-symmetric-45	[45, − 45, 0, 45, − 45]	$A_{11} \neq 0, A_{12} \neq 0, A_{22} \neq 0, A_{66} \neq 0, A_{16} = 0, A_{26} = 0$ $B_{11} = 0, B_{12} = 0, B_{22} = 0, B_{66} = 0, B_{16} \neq 0, B_{26} \neq 0$ $D_{11} \neq 0, D_{12} \neq 0, D_{22} \neq 0, D_{66} \neq 0, D_{16} = 0, D_{26} = 0$

The accuracy of the developed method was verified by comparing it to the finite element method. Close agreement is demonstrated between the results of the developed method and those of the finite element method in terms of central deflection. However, there is a quiet difference in magnitude of the stresses at the plate's center [7]. Wang et al. also investigated the dynamic response of composite plates utilizing the finite strip method, but under different types of loads, stepped, triangular, sinusoidal, and blast loading. Further the study investigated different boundary conditions [8]. Ganapathi et al. developed an eight-node finite element that accounts for the in-plane and transverse displacement through thickness by employing the zigzag function. The results obtained from the developed theory were compared and proved to be more accurate than the first-order and higher-order shear deformation theory [9]. Amabili et al. explored the nonlinear response to a harmonic excitation in the vicinity of the fundamental mode. They concluded that for thick plates it is recommended to use shear deformation theories, and for thin plates it is recommended to use

3962, 2026, 1, Downloaded from https://onlinelibrary.wiley.com/doi/10.1155/je/9725460 by Turkey Cochrane Evidence Aid, Wiley Online Library on [01/10/2026]. See the Terms and Conditions (https://onlinelibrary.wiley.com/terms-and-conditions) on Wiley Online Library for rules of use; OA articles are governed by the applicable Creative Commons License

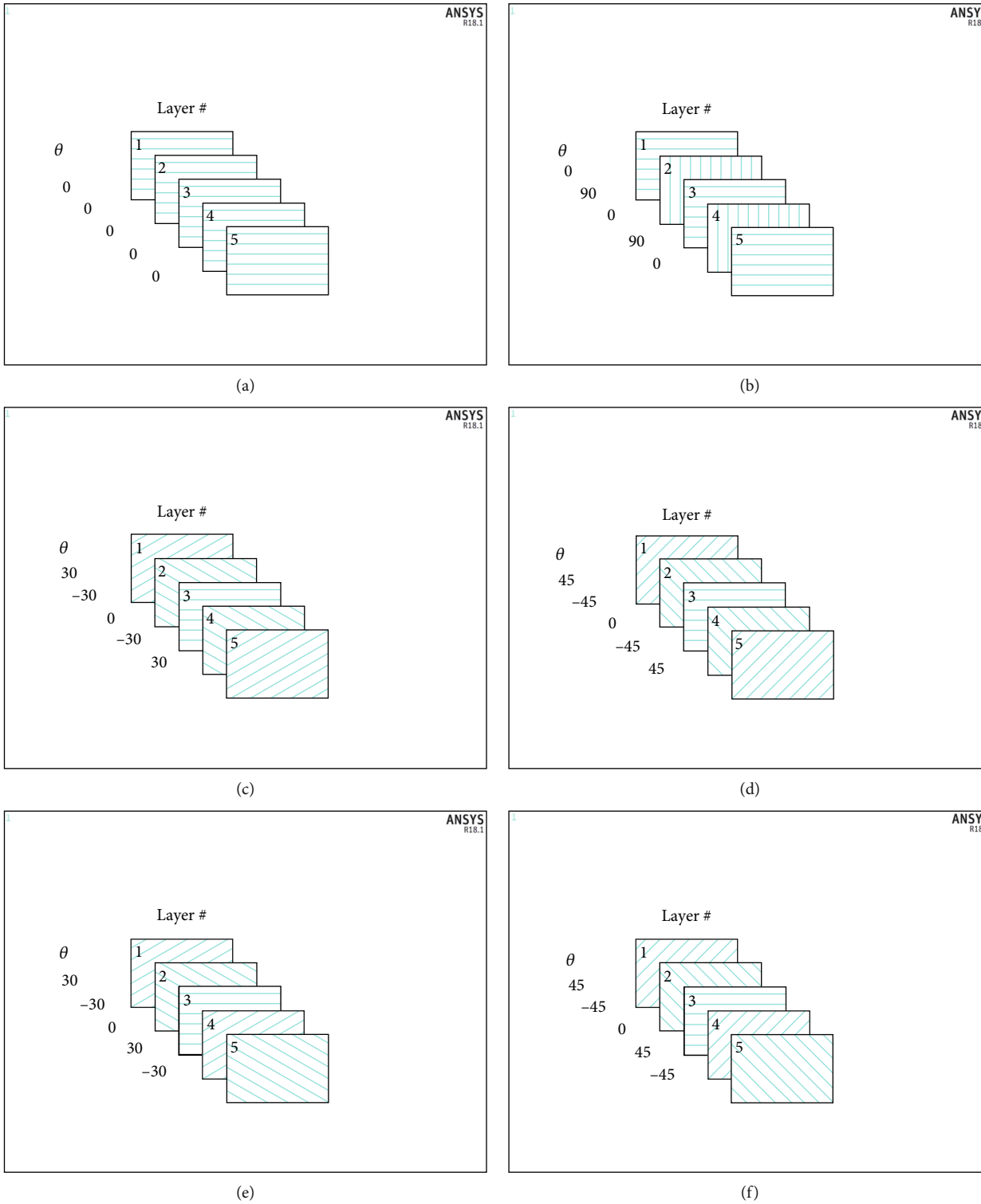


FIGURE 2: Stacking sequences of all models. (a) Unidirectional. (b) Balanced cross-ply. (c,d) Symmetric angled-ply. (e,f) Anti-symmetric angled-ply.

Von-Karman [10]. Amabili et al. extended the research by utilizing different solution techniques, the pseudo-arclength continuation method and bifurcation analysis. Further, the study considered different boundary conditions. The results showed large differences in the results obtained from Von-Karman, first-order, and third-order deformation theories for thick plates, but concise for thin plates [11]. Kazanci et al. conducted a parametric study on the nonlinear dynamic behavior of composite plates by considering the aspect ratio, fiber orientation and layer number. The

3962, 2026, 1, Downloaded from https://onlinelibrary.wiley.com/doi/10.1155/je/9725460 by Turkey Cochrane Evidence Aid, Wiley Online Library on [01/10/2026]. See the Terms and Conditions (https://onlinelibrary.wiley.com/terms-and-conditions) on Wiley Online Library for rules of use; OA articles are governed by the applicable Creative Commons License

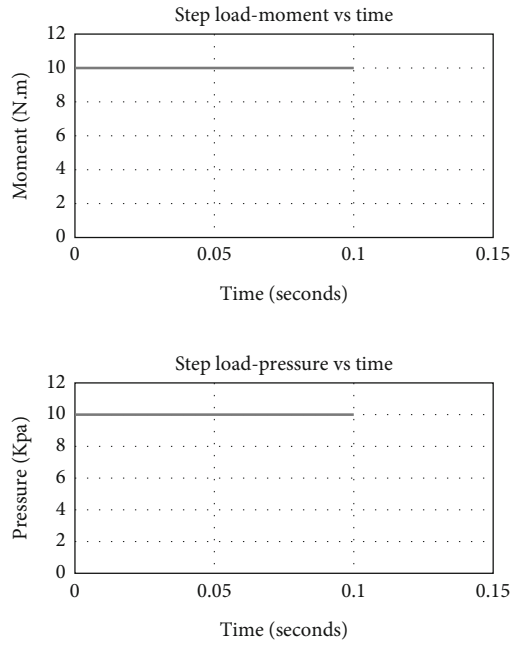


Figure 3: Step loads applied, pressure and moment.

TABLE 3: Solution convergence analysis at mid-node.

Laminate	10 × 10 mesh size, 100 element	20 × 20 mesh size, 400 elements	50 × 50 mesh size, 2500 elements	100 × 100 mesh size, 10,000 elements	Error%
Unidirectional	0.333e−3	0.664e−3	1.637e−3	1.609e−3	1.71
Cross-ply	0.239e−3	0.459e−3	1.116e−3	1.145−3	2.60
Symmetric-30	0.450e−3	0.874e−3	2.121e−3	2.069e−3	2.45
Symmetric-45	0.338e−3	0.728e−3	1.730e−3	1.693e−3	2.14
Anti-sym.-30	1.024e−3	1.988e−3	2.262e−3	2.208e−3	2.39
Anti-sym.-45	0.785e−3	1.514e−3	1.829e−3	1.778e−3	2.79

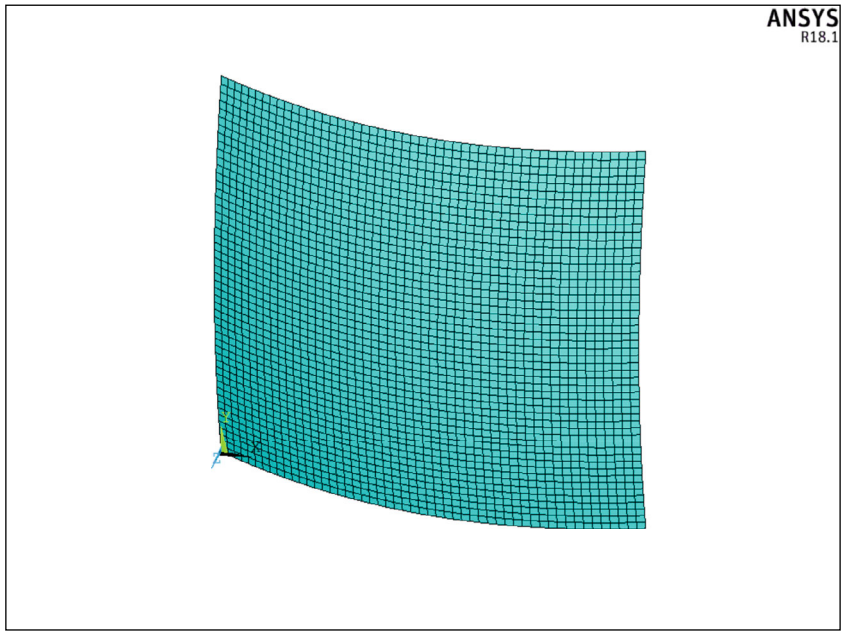


Figure 4: Finite element model.

3962, 2026, 1, Downloaded from https://onlinelibrary.wiley.com/doi/10.1155/je/9725460 by Turkey Cochrane Evidence Aid, Wiley Online Library on [01/10/2026]. See the Terms and Conditions (https://onlinelibrary.wiley.com/terms-and-conditions) on Wiley Online Library for rules of use; OA articles are governed by the applicable Creative Commons License

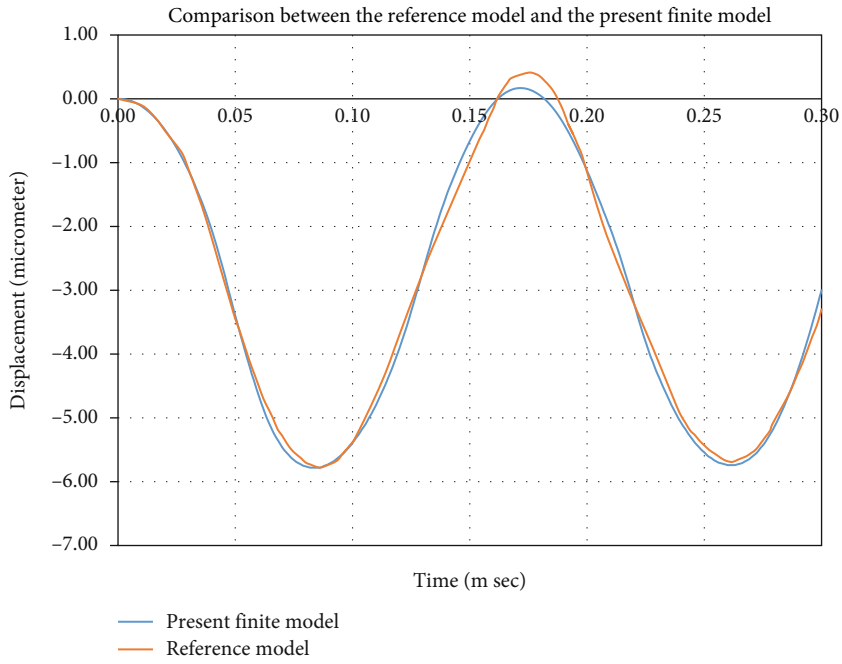


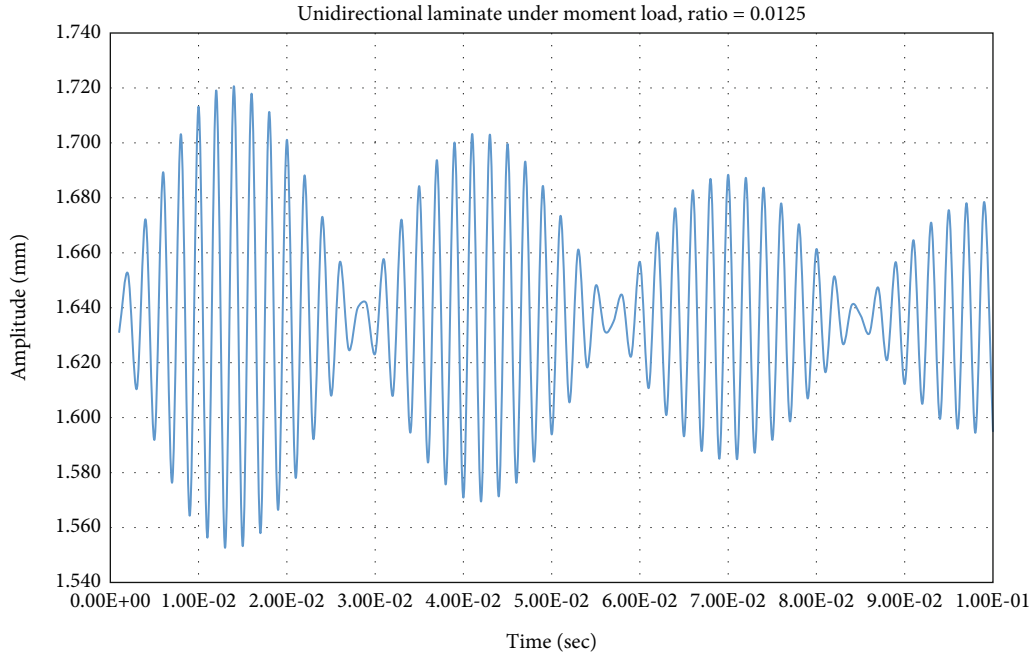
Figure 5: Central deflection of the reference model [30].

TABLE 4: Models investigated in the analysis.

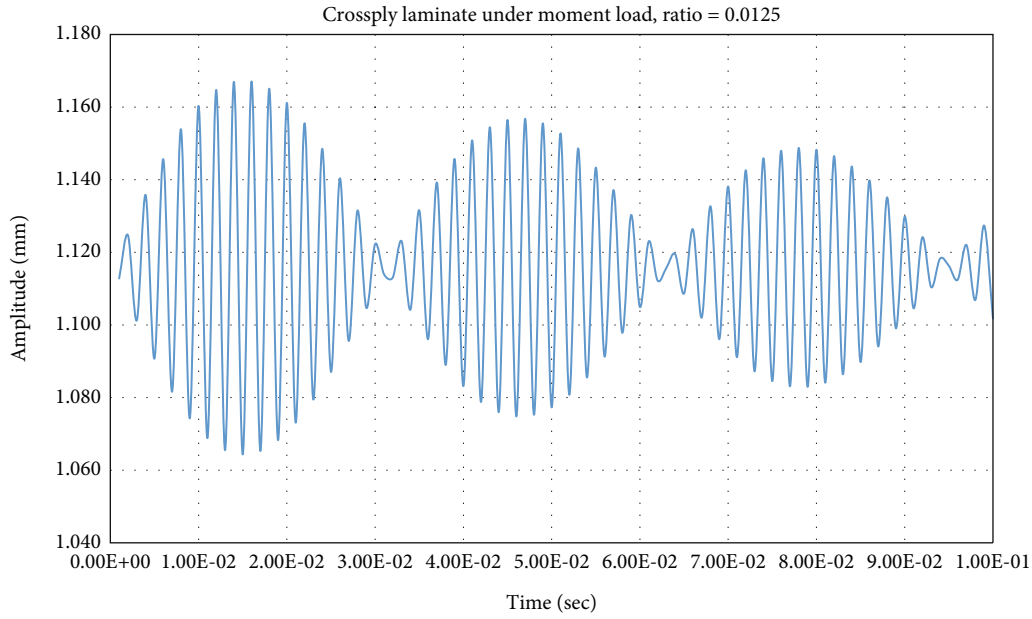
Name	Stacking	Load	Thickness/length
Unidirectional	[0, 0, 0, 0, 0]	Moment/pressure	0.0125/0.025/0.0375
Cross-ply	[0, 90, 0, 90, 0]	Moment/pressure	0.0125/0.025/0.0375
Symmetric-30	[30, − 30, 0, − 30, 30]	Moment/pressure	0.0125/0.025/0.0375
Symmetric-45	[45, − 45, 0, − 45, 45]	Moment/pressure	0.0125/0.025/0.0375
Anti-symmetric-30	[30, -30, 0, 30, -30]	Moment/pressure	0.0125/0.025/0.0375
Anti-symmetric-45	[45, − 45, 0, 45, − 45]	Moment/pressure	0.0125/0.025/0.0375

equations of motion were derived based on the virtual work principle, and the finite difference method is applied to solve the system. Fiber orientation has no effect on the vibration characteristics of a cross-ply laminate. As the aspect ratio decreases, vibration amplitude decreases. However, vibration frequency increases if layer number decreases [12]. Kazanci et al. extended their work by considering a time-dependent pulse load. Though, no substantial differences in the behavior from the behavior of the previous study [13]. Continuing with the same theoretical framework and methodology, Baştürk et al. investigated the nonlinear dynamic response of hybrid laminated plates incorporating the effect of damping into their analysis [14]. Khandelwal et al. made a broad study on the shear deformation theories focusing on the effects of shear strain variations through thickness, on free and forced plates' response. The developed finite element efficiently modeled the imperfections at the layer interface [15]. Kazanci conducted a broad review focused on the studies of the response of laminated composite plates under blast loading. In this review, they traced the chronological development of the theories related to composite laminates, describing the hypothesis, mathematics, displacements functions, linearity and nonlinearity, coupled and uncoupled, damping effects, accuracy, analytical and numerical solutions [16]. Shao et al. developed a unified and analytical solution for the transient response of cross-ply composite laminated rectangular plates with general boundary restraints. The analytical solution is derived by means of the method of reverberation ray matrix. The accuracy of the proposed solution was validated by results obtained from finite element analysis [17]. From design perspective, it is important to keep the deflection of composites within certain accepted range. Stiffeners made of sandwich plates are often used as an effective solution. Balkan et al. studied the effect of sandwich stiffeners on the dynamic response of composite plates under nonuniform blast loading. A decrease in maximum displacement and failure index of the plate was observed with increasing thickness and width of the stiffener [18]. Pratico et al. were the first to publish a study on the dynamic and vibrations of curve linearly substiffened plates. The curve patterns were purposely chosen in order to investigate the directional properties and how they change for different stiffener curvature value. Which the study confirmed to be the case [19]. Akour et al.

3962, 2026, 1, Downloaded from https://onlinelibrary.wiley.com/doi/10.1155/je/9725460 by Turkey Cochrane Evidence Aid, Wiley Online Library on [01/10/2026]. See the Terms and Conditions (https://onlinelibrary.wiley.com/terms-and-conditions) on Wiley Online Library for rules of use; OA articles are governed by the applicable Creative Commons License



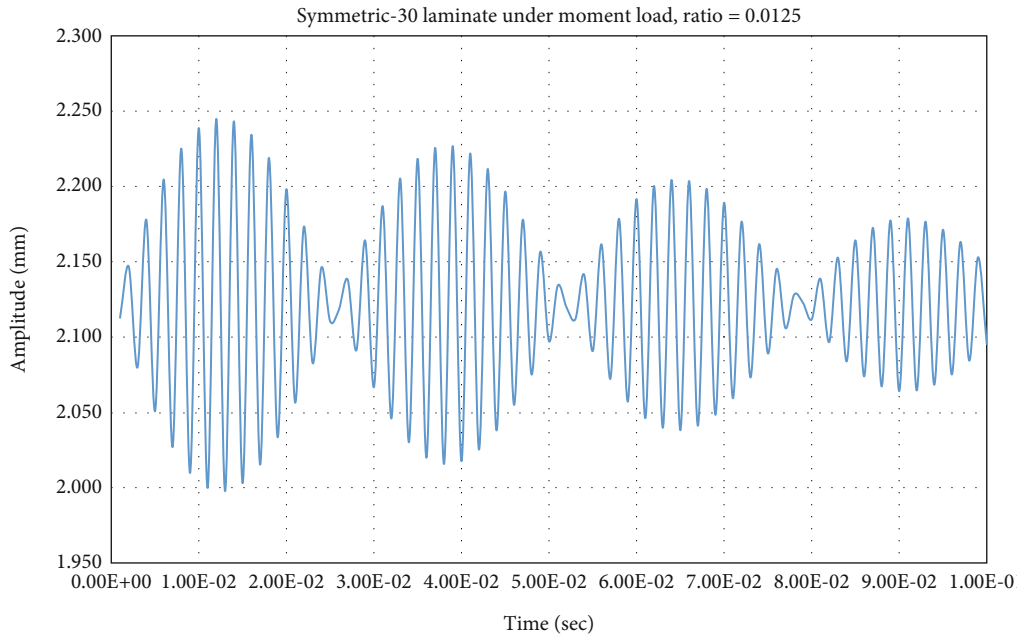
(a)



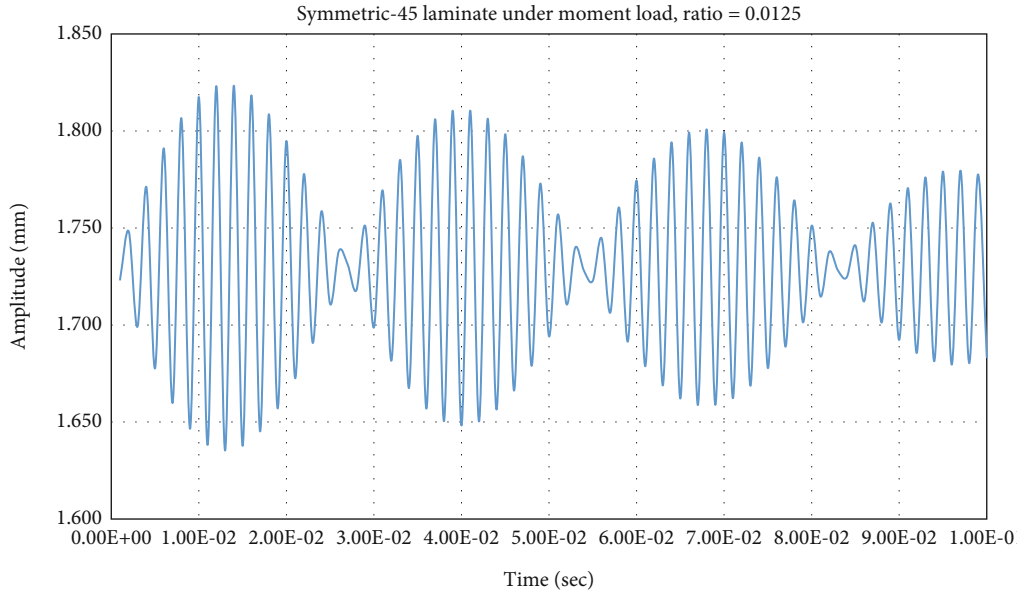
(b)

Figure 6: Continued.

3962, 2026, 1, Downloaded from https://onlinelibrary.wiley.com/doi/10.1155/je/9725460 by Turkey Cochrane Evidence Aid, Wiley Online Library on [01/10/2026]. See the Terms and Conditions (https://onlinelibrary.wiley.com/terms-and-conditions) on Wiley Online Library for rules of use; OA articles are governed by the applicable Creative Commons License



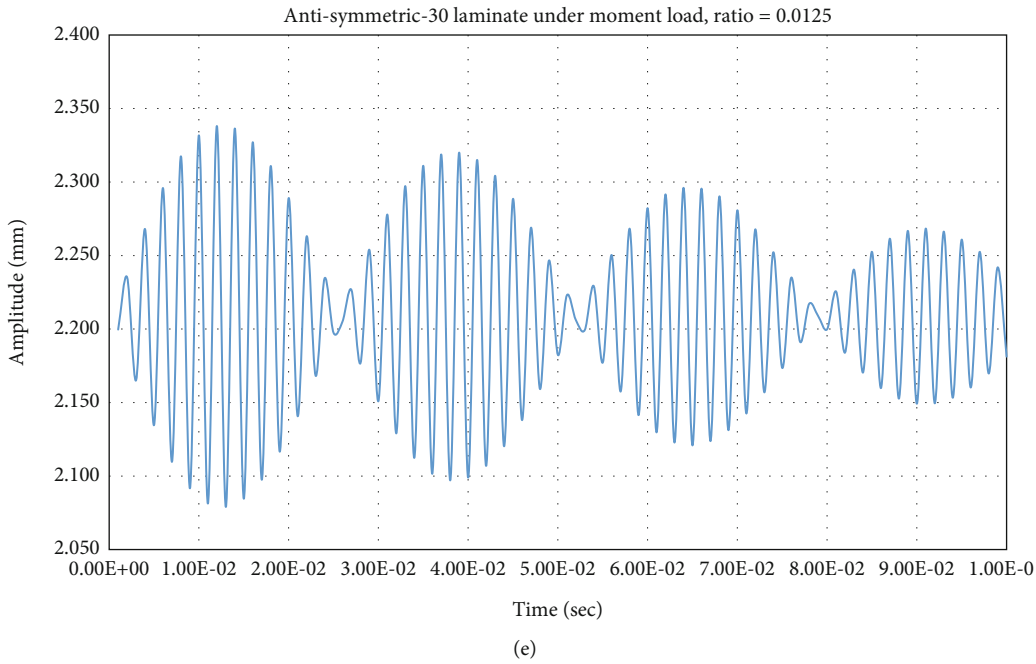
(c)



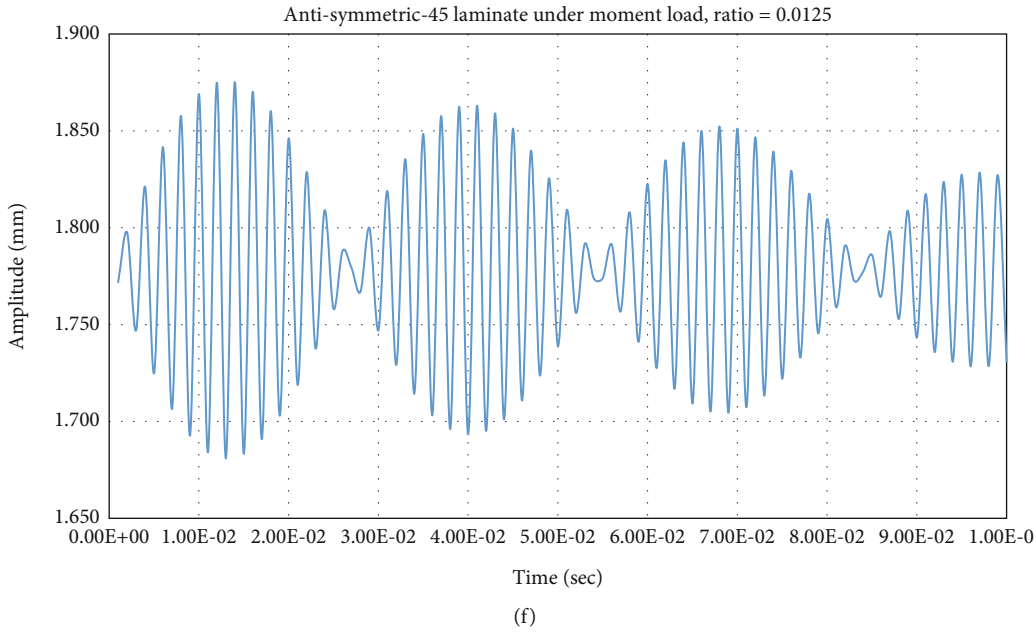
(d)

Figure 6: Continued.

3962, 2026, 1, Downloaded from https://onlinelibrary.wiley.com/doi/10.1155/je/9725460 by Turkey Cochrane Evidence Aid, Wiley Online Library on [01/10/2026]. See the Terms and Conditions (https://onlinelibrary.wiley.com/terms-and-conditions) on Wiley Online Library for rules of use; OA articles are governed by the applicable Creative Commons License



(e)

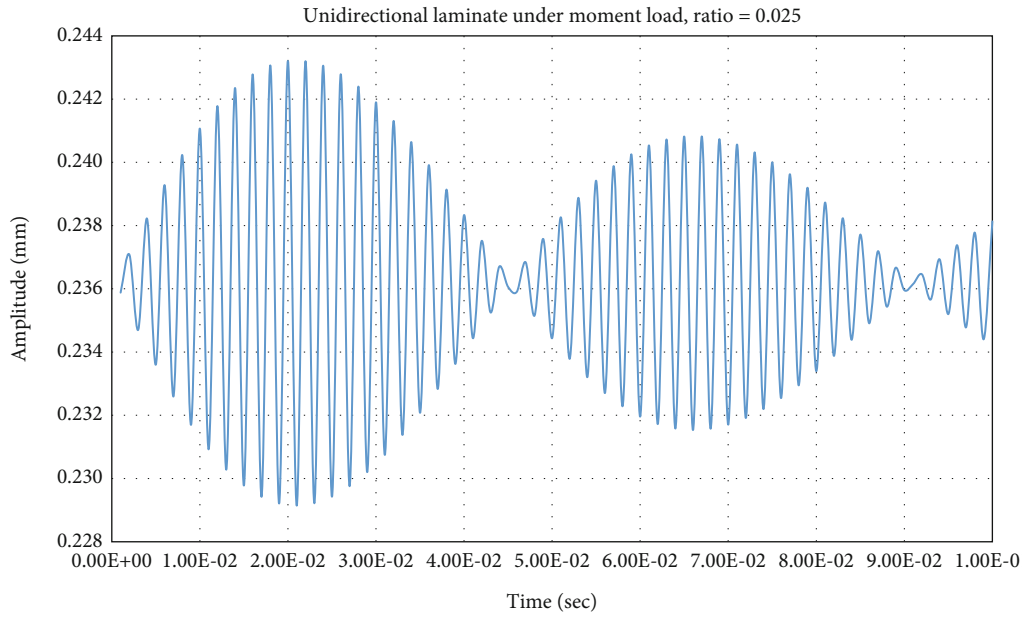


(f)

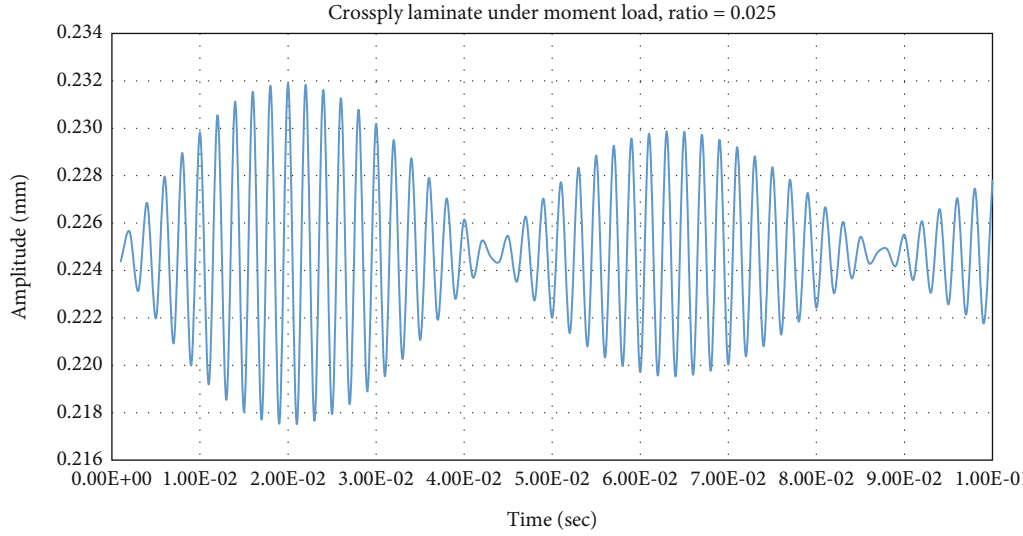
Figure 6: Dynamic response of (a) unidirectional, (b) cross-ply, (c) symm-30, (d) symm-45, (e) anti-30, (f) anti-45 laminates under moment loading (ratio 0.0125).

investigated the transverse displacement of simply supported plates due to thermal induction. The transverse displacement is obtained by the superposition of the quasi-static first mode, which is obtained by Levy-type solution, and the dynamic solution, which is based on the classical laminate theory. The results showed that the dynamic response of unidirectional and cross-ply laminates are similar in terms of the shape of the response only and are affected by the thickness only. The anti-symmetric angle-ply laminates exhibit differences in the response based on the fiber orientation [20]. Akour continued the research by investigating the dynamic response of simply supported composite plates subjected to sudden heat flux using the finite element method. It was demonstrated that neglecting the coupling between the induced moments and in-plane loads in anti-symmetric cross-ply laminates will yield deceptive results [21]. Further extending the research, thin square laminated composite plates that are balanced and simply supported were investigated using the finite element method. However, the focus was on how the interactions of the constituent materials' stiffness contributed to the dynamic response. Considering different stacking sequences, it was observed

3962, 2026, 1, Downloaded from https://onlinelibrary.wiley.com/doi/10.1155/je/9725460 by Turkey Cochrane Evidence Aid, Wiley Online Library on [01/10/2026]. See the Terms and Conditions (https://onlinelibrary.wiley.com/terms-and-conditions) on Wiley Online Library for rules of use; OA articles are governed by the applicable Creative Commons License



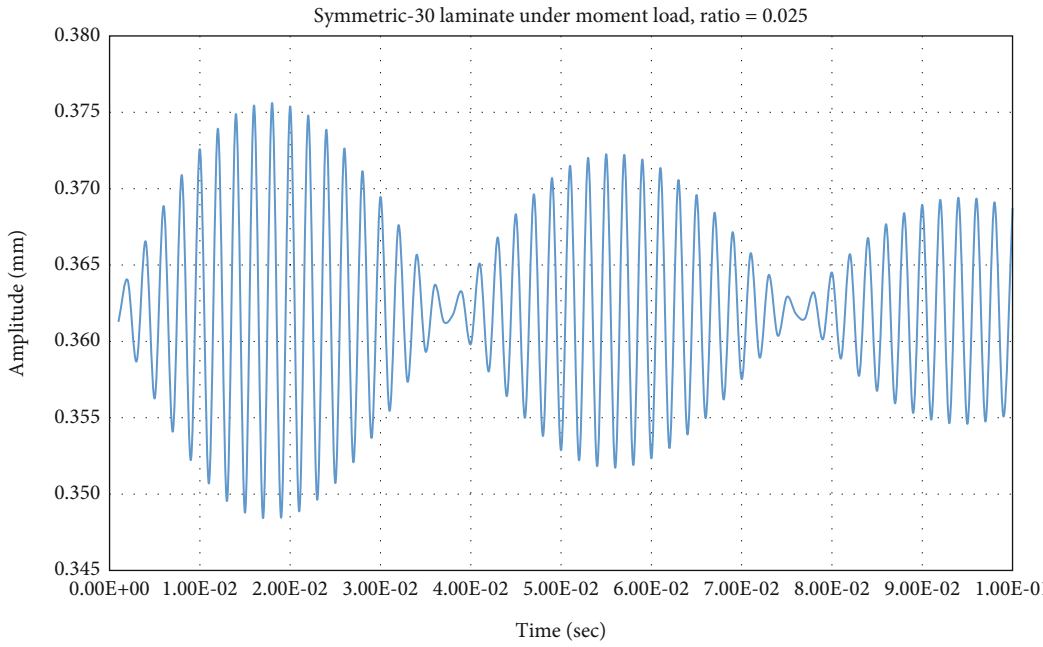
(a)



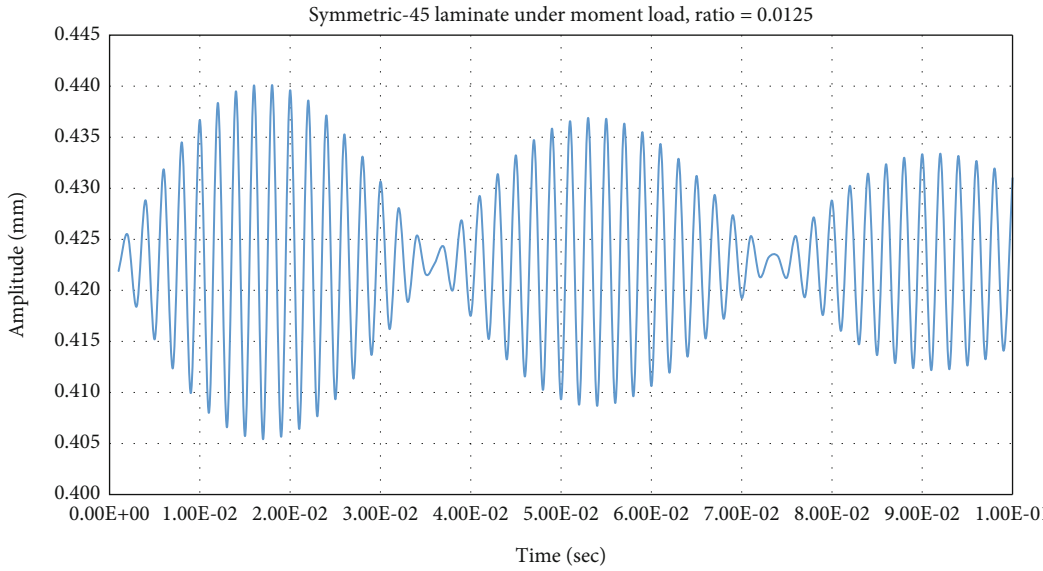
(b)

Figure 7: Continued.

3962, 2026, 1, Downloaded from https://onlinelibrary.wiley.com/doi/10.1155/je/9725460 by Turkey Cochrane Evidence Aid, Wiley Online Library on [01/10/2026]. See the Terms and Conditions (https://onlinelibrary.wiley.com/terms-and-conditions) on Wiley Online Library for rules of use; OA articles are governed by the applicable Creative Commons License



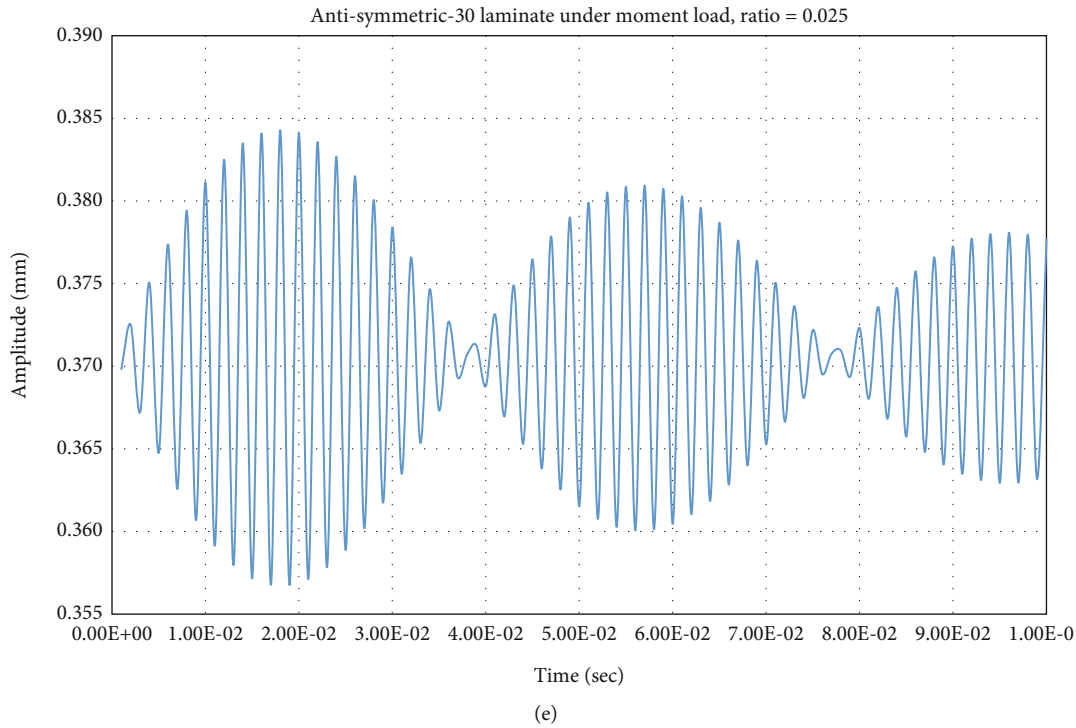
(c)



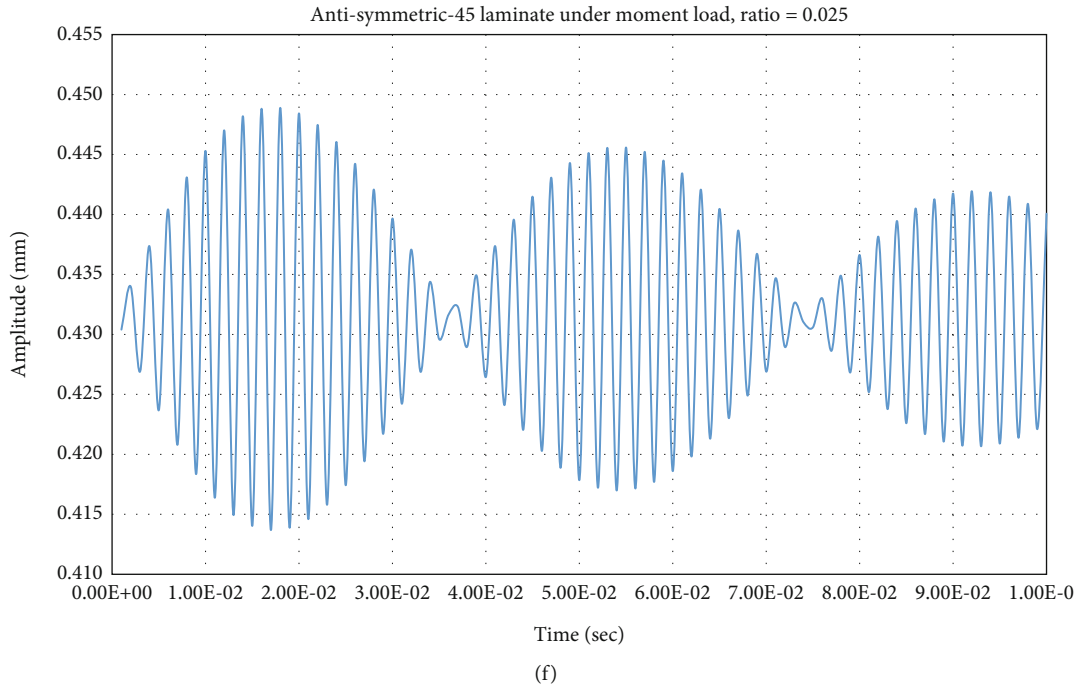
(d)

Figure 7: Continued.

3962, 2026, 1, Downloaded from https://onlinelibrary.wiley.com/doi/10.1155/je/9725460 by Turkey Cochrane Evidence Aid, Wiley Online Library on [01/10/2026]. See the Terms and Conditions (https://onlinelibrary.wiley.com/terms-and-conditions) on Wiley Online Library for rules of use; OA articles are governed by the applicable Creative Commons License



(e)

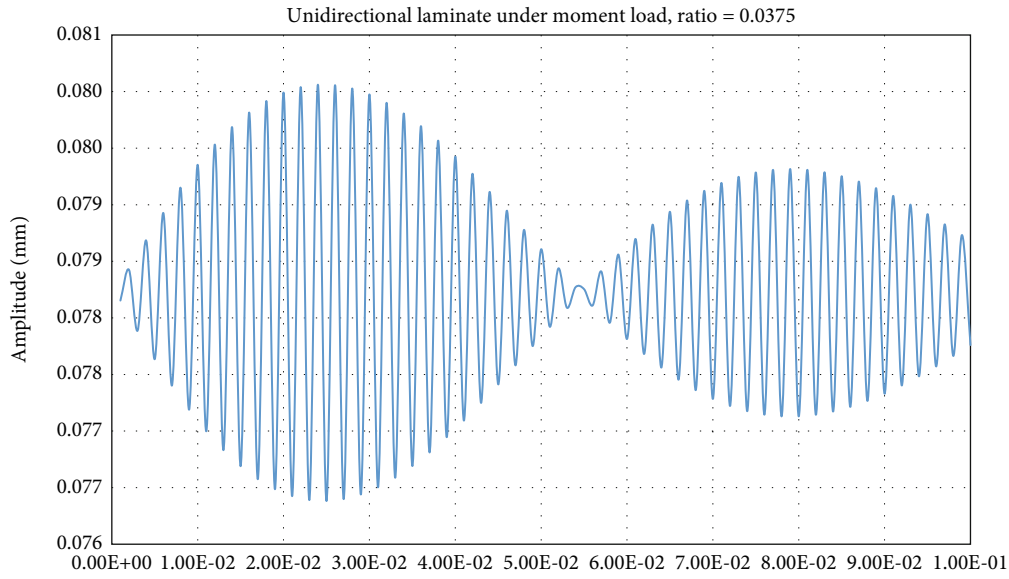


(f)

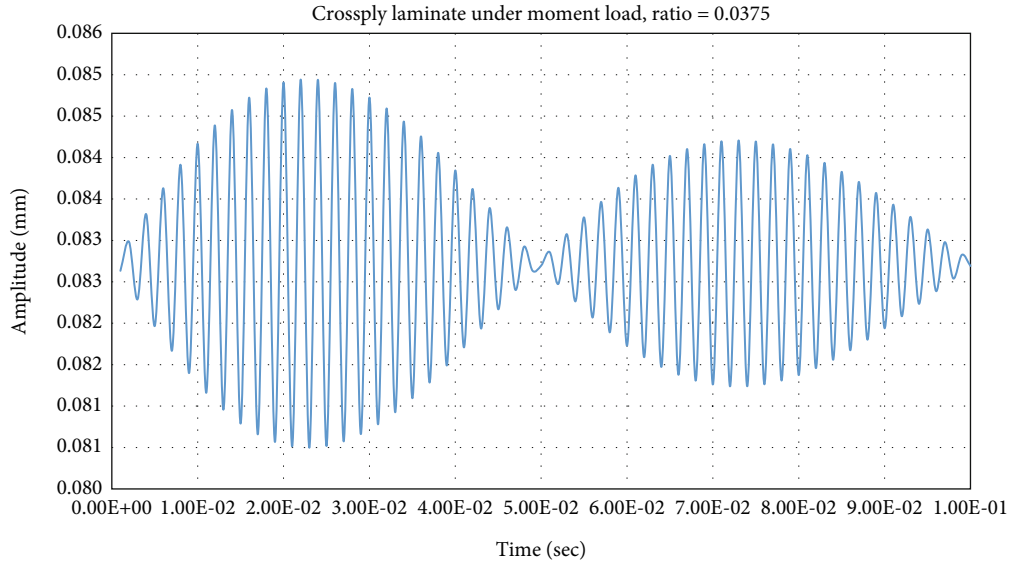
FIGURE 7: Dynamic response of (a) unidirectional, (b) cross-ply, (c) symm-30, (d) symm-45, (e) anti-30, (f) anti-45 laminates under moment loading (ratio 0.025).

that all cases investigated are amplitude modulated [22]. Isfahani et al. investigated the effects of adding various nanoparticles to glass fiber reinforced polymer composites. Low velocity impact tests showed that multi-walled carbon nanotubes resulted in lower contact forces and full rebound. Indicating minimal damage [23]. Xie et al. developed a nonlinear analytical model to study the low-velocity impact of a sandwich plate with an auxetic honeycomb-core layer. The auxetic were derived using a homogenization method to express effective material coefficients based on material properties and cellular geometry. The model was validated against existing literature, followed by numerical analyses exploring how cellular geometry and impactor conditions, such as velocity, mass, and nose curvature affects the nonlinear dynamic

3962, 2026, 1, Downloaded from https://onlinelibrary.wiley.com/doi/10.1155/je/9725460 by Turkey Cochrane Evidence Aid, Wiley Online Library on [01/10/2026]. See the Terms and Conditions (https://onlinelibrary.wiley.com/terms-and-conditions) on Wiley Online Library for rules of use; OA articles are governed by the applicable Creative Commons License



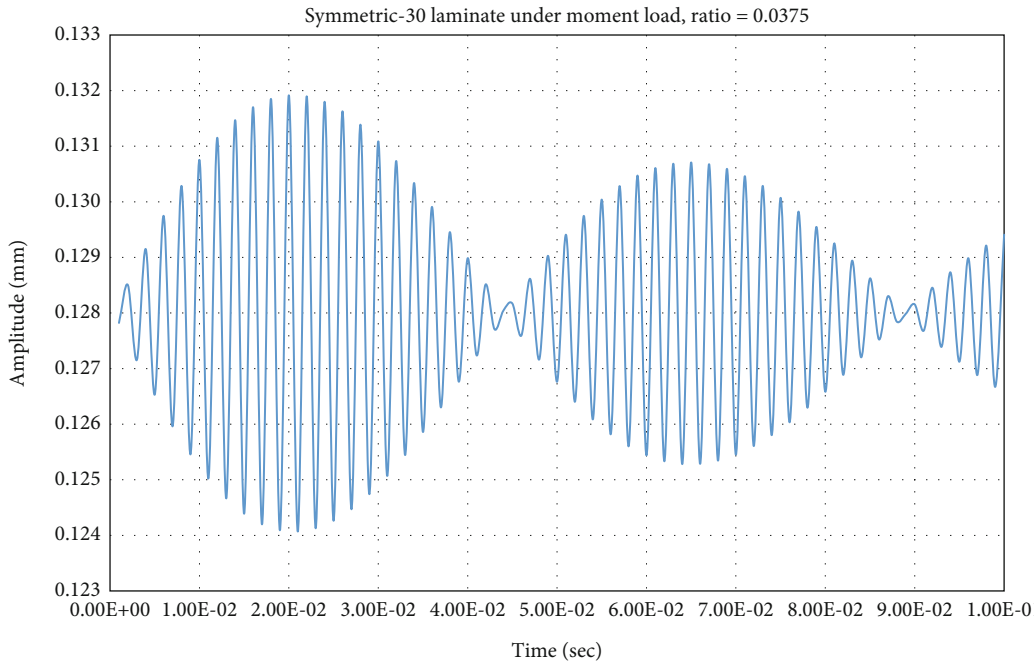
(a)



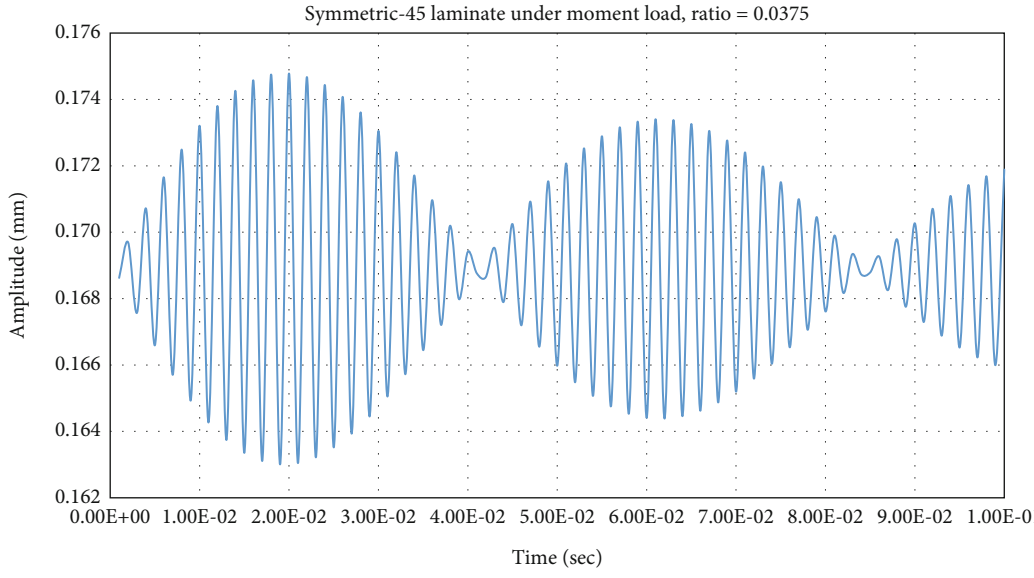
(b)

Figure 8: Continued.

3962, 2026, 1, Downloaded from https://onlinelibrary.wiley.com/doi/10.1155/je/9725460 by Turkey Cochrane Evidence Aid, Wiley Online Library on [01/10/2026]. See the Terms and Conditions (https://onlinelibrary.wiley.com/terms-and-conditions) on Wiley Online Library for rules of use; OA articles are governed by the applicable Creative Commons License



(c)



(d)

Figure 8: Continued.

3962, 2026, 1, Downloaded from https://onlinelibrary.wiley.com/doi/10.1155/je/9725460 by Turkey Cochrane Evidence Aid, Wiley Online Library on [01/10/2026]. See the Terms and Conditions (https://onlinelibrary.wiley.com/terms-and-conditions) on Wiley Online Library for rules of use; OA articles are governed by the applicable Creative Commons License

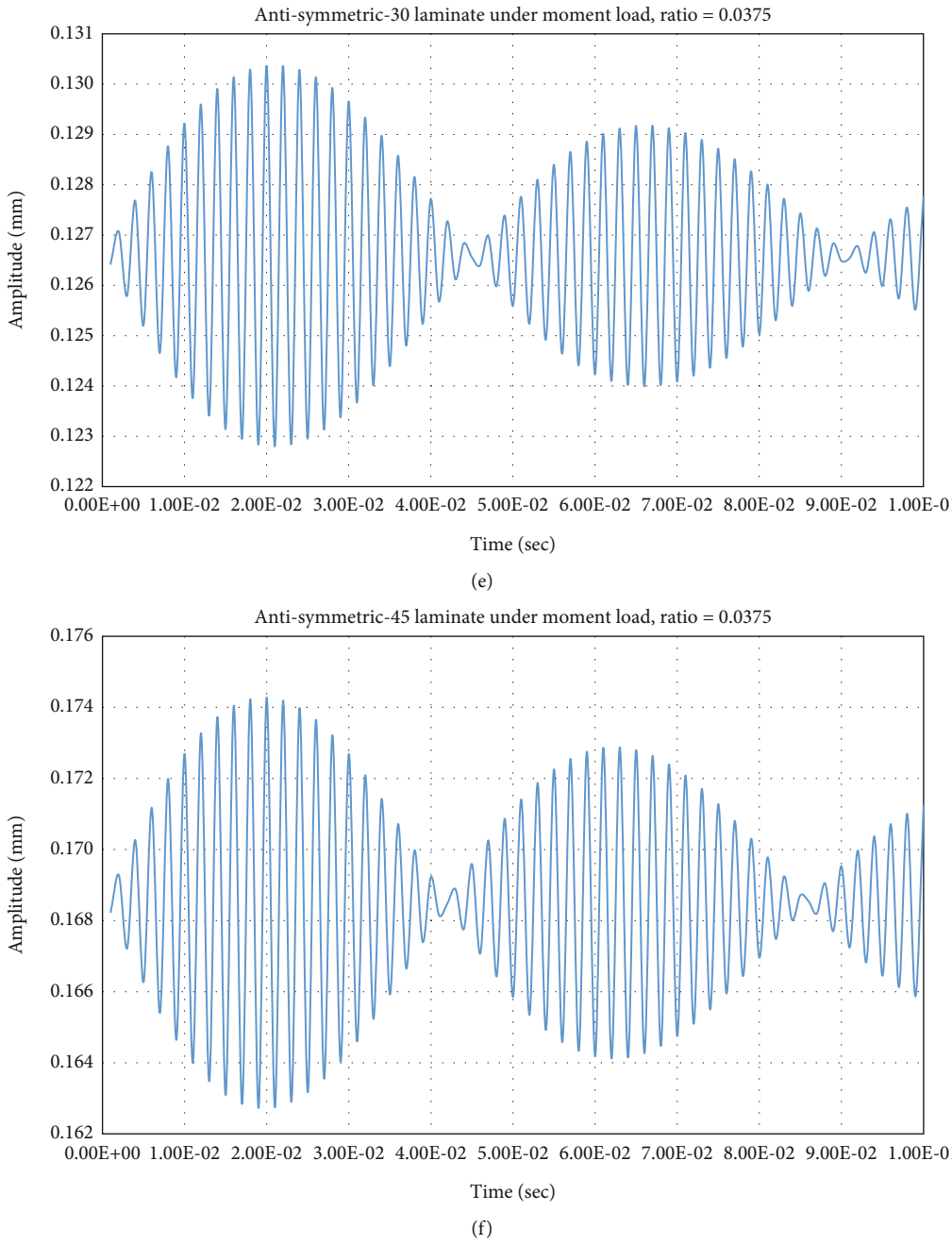


Figure 8: Dynamic response of (a) unidirectional, (b) cross-ply, (c) symm-30, (d) symm-45, (e) anti-30, (f) anti-45 laminates under moment loading (ratio 0.0375).

response. The results showed that these factors significantly influence the system's collision impact behavior [24].

Research on curved composite plates demonstrates their complex mechanical behavior, which is highly dependent on their geometry and layer orientation. Studies show that the curvature significantly influences buckling resistance and free vibration characteristics, with specific layup sequences being crucial for optimizing structural stability. Furthermore, the dynamic response, including how these curved plates vibrate and respond to impacts, is distinctly different from flat panels, requiring specialized analytical and finite element models to accurately predict their performance and failure modes for advanced engineering applications [25–27].

1.1. Motivation. The use of laminated composite plates in aerospace and defense applications, particularly in low-observable platforms, demands a thorough understanding of their dynamic behavior. These structures are subjected to sudden dynamic loads from maneuvers, gusts, or shockwaves, which can induce complex vibrational responses. This study investigates the control of these transient vibrations in simply supported spherical composite plates.

3962, 2026, 1, Downloaded from https://onlinelibrary.wiley.com/doi/10.1155/je/9725460 by Turkey Cochrane Evidence Aid, Wiley Online Library on [01/10/2026]. See the Terms and Conditions (https://onlinelibrary.wiley.com/terms-and-conditions) on Wiley Online Library for rules of use; OA articles are governed by the applicable Creative Commons License

TABLE 5: Summary results of average and maximum displacement of laminates under moment loading.

Stacking	Thickness/length	Average/thickness	Maximum/thickness	Deformation range(mm)
Unidirectional	0.0125	1.309	1.376	0.168
Cross-ply	0.0125	0.893	0.943	0.104
Symmetric-30	0.0125	1.697	1.795	0.247
Symmetric-45	0.0125	1.383	1.458	0.188
Anti-symmetric-30	0.0125	1.766	1.870	0.259
Anti-symmetric-45	0.0125	1.422	1.500	0.194
Unidirectional	0.025	0.094	0.097	0.0141
Cross-ply	0.025	0.089	0.092	0.0144
Symmetric-30	0.025	0.144	0.150	0.0272
Symmetric-45	0.025	0.169	0.176	0.0283
Anti-symmetric-30	0.025	0.148	0.153	0.0275
Anti-symmetric-45	0.025	0.172	0.179	0.0352
Unidirectional	0.0375	0.0209	0.0213	3.680
Cross-ply	0.0375	0.0221	0.0227	4.444
Symmetric-30	0.0375	0.0341	0.0352	7.847
Symmetric-45	0.0375	0.0450	0.0466	11.18
Anti-symmetric-30	0.0375	0.0338	0.0348	7.566
Anti-symmetric-45	0.0375	0.0449	0.0465	11.55

The practical motivation is two-fold. First, and most directly, excessive vibration can compromise the precise geometric integrity of a stealthy airframe, which is critical for maintaining its low radar cross section. Our findings demonstrate how designers can use stacking sequence and thickness as "amplitude knobs" to suppress this deformation.

Second, beyond gross deformation, the high-frequency vibrational modes of a structure can impose a micro-Doppler signature on reflected radar waves, which can be exploited by advanced signal processing for target identification. While this study does not investigate the electromagnetic scattering itself, it provides a foundational understanding for controlling the underlying structural vibrations. By demonstrating that key design parameters significantly affect the amplitude of the dynamic response without altering its frequency characteristics, this work lays the groundwork for future research into vibration-stealth co-design. This could lead to structures whose mechanical dynamic properties are optimized not only for structural performance but also for minimizing detectable vibrational signatures.

1.2. Research Gap. The primary research gap this study addresses is the lack of a comprehensive understanding of how specific design parameters *independently* control the amplitude and frequency characteristics of the dynamic response in spherical laminated composite plates under sudden loading.

Previous research likely understood that parameters like stacking sequence, thickness, and load type affect the overall dynamic response. However, this study systematically uncovers a more nuanced relationship: These parameters can be used to selectively control only the amplitude of the response without altering its natural frequency.

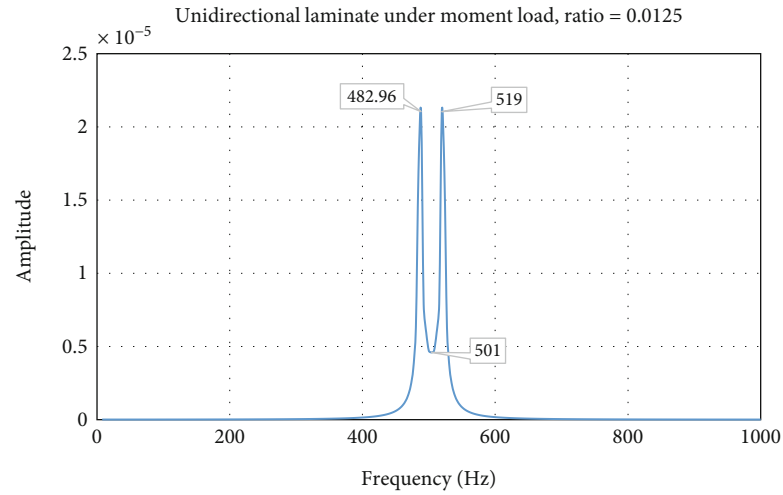
1.3. Objective. In this study, the dynamic response of simply supported spherically curved laminated composite plate of different stacking's, different aspect ratios, and different types of loading is investigated. In this research, the nature of the response, the amplitude and frequency characteristics of the plate are affected by fiber orientation, aspect ratio, and type of loading are explored.

2. Methodology and Finite Element Model

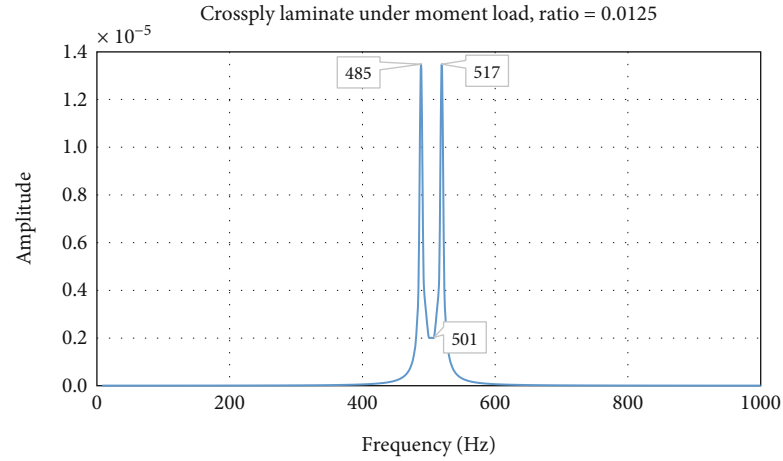
The physical model utilized in the analysis is a simply supported composite plate. The laminate consists of five layers arranged in six different stacking sequences: unidirectional, cross-ply, symmetrical, and anti-symmetric laminate. Three different thicknesses to length ratios are considered, 0.0125, 0.025, and 0.0375, and two types of loading are considered, surface pressure and moment on edges. The constituent materials are graphite and epoxy.

2.1. Geometry. The laminate can be described as a square shaped, spherically curved simply supported plate. The dimensions from vertex to vertex is 0.1 m and the thickness is varied as a parameter to study its influence. Three thickness to length ratio were considered, 0.0125, 0.025, and 0.0375. Noting that despite thickness variation, the laminate still satisfies thin laminate plate conditions. The plate's radius of curvature is 2.5 m. The model is curved to investigate the effect of curvature on the laminate's response and comparing it to the findings of Akour [22] for flat plates. The large curvature radius relative to the plate thickness and lateral dimensions is intended to allow the plate to be treated as a flat plate as an approximation, to justify using the natural frequency equation for flat plates to calculate

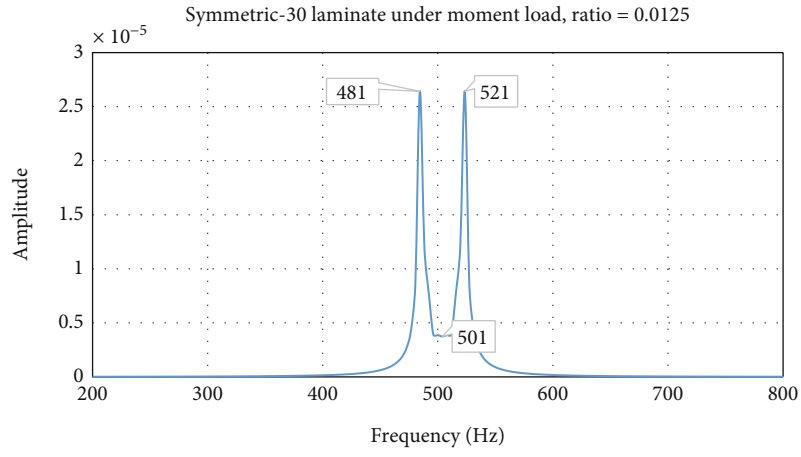
3962, 2026, 1, Downloaded from https://onlinelibrary.wiley.com/doi/10.1155/je/9725460 by Turkey Cochrane Evidence Aid, Wiley Online Library on [01/10/2026]. See the Terms and Conditions (https://onlinelibrary.wiley.com/terms-and-conditions) on Wiley Online Library for rules of use; OA articles are governed by the applicable Creative Commons License



(a)



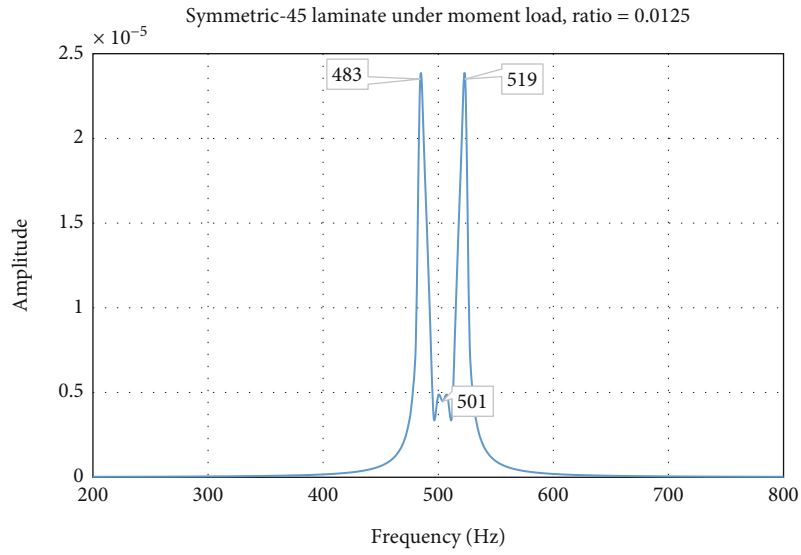
(b)



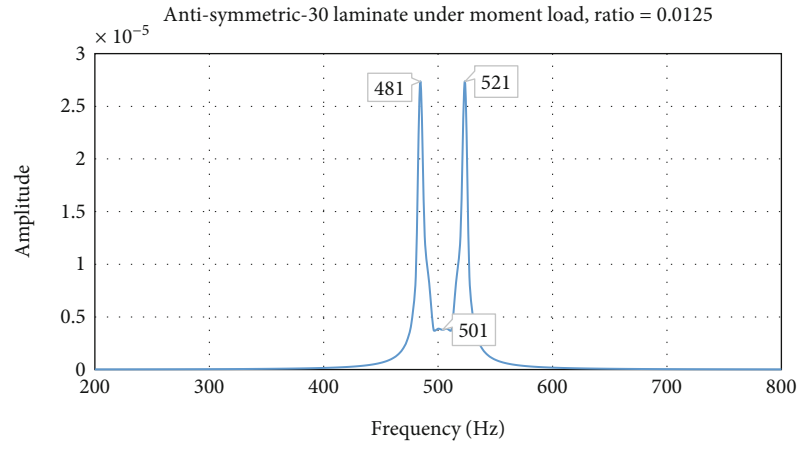
(c)

Figure 9: Continued.

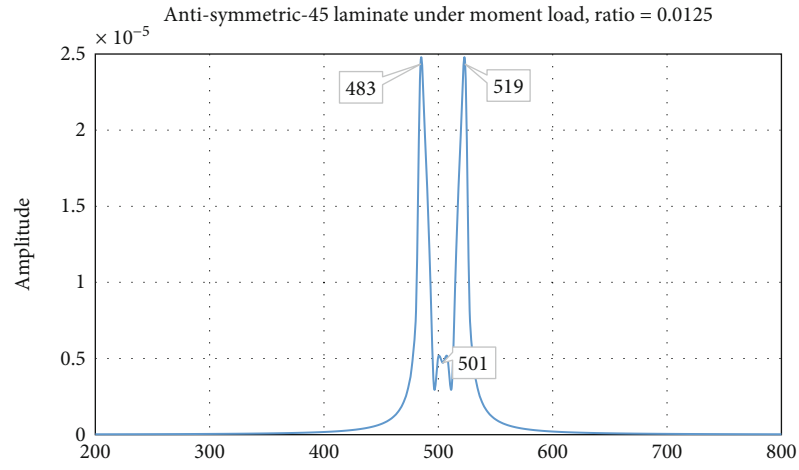
3962, 2026, 1, Downloaded from https://onlinelibrary.wiley.com/doi/10.1155/je/9725460 by Turkey Cochrane Evidence Aid, Wiley Online Library on [01/10/2026]. See the Terms and Conditions (https://onlinelibrary.wiley.com/terms-and-conditions) on Wiley Online Library for rules of use; OA articles are governed by the applicable Creative Commons License



(d)



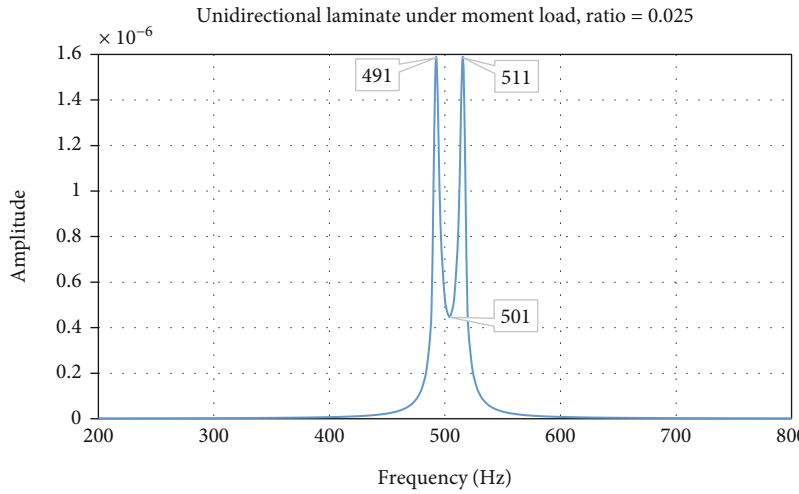
(e)



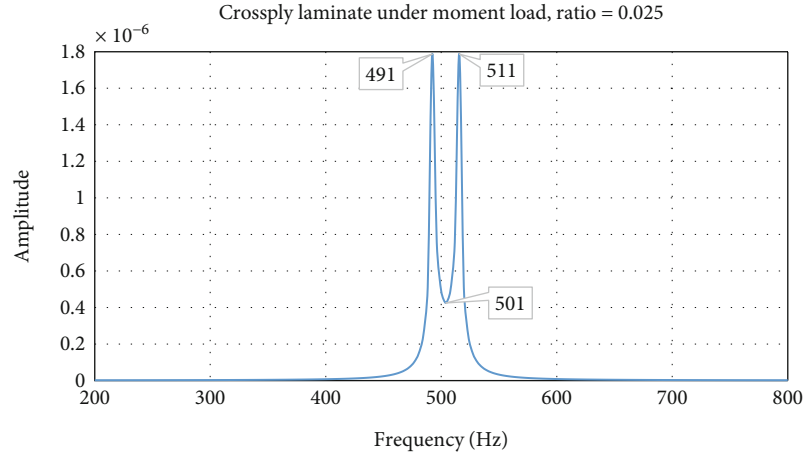
(f)

Figure 9: Fourier analysis of (a) unidirectional, (b) cross-ply, (c) symm-30, (d) symm-45, (e) anti-30, (f) anti-45 laminates under moment loading (ratio 0.0125).

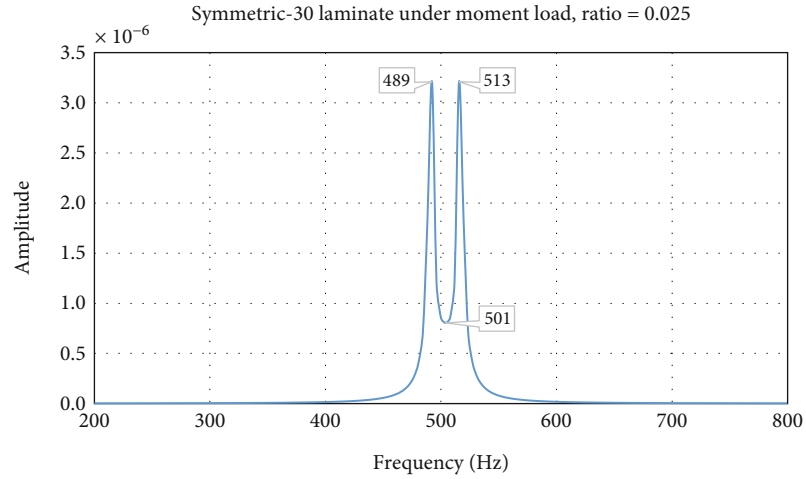
3962, 2026, 1, Downloaded from https://onlinelibrary.wiley.com/doi/10.1155/je/9725460 by Turkey Cochrane Evidence Aid, Wiley Online Library on [01/10/2026]. See the Terms and Conditions (https://onlinelibrary.wiley.com/terms-and-conditions) on Wiley Online Library for rules of use; OA articles are governed by the applicable Creative Commons License



(a)



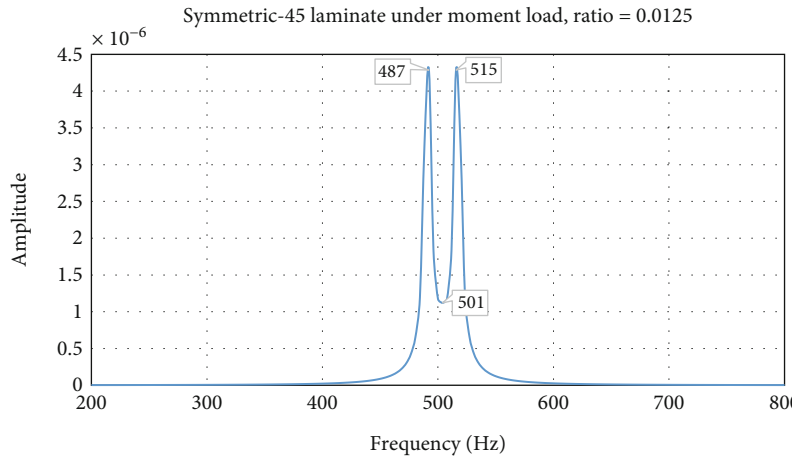
(b)



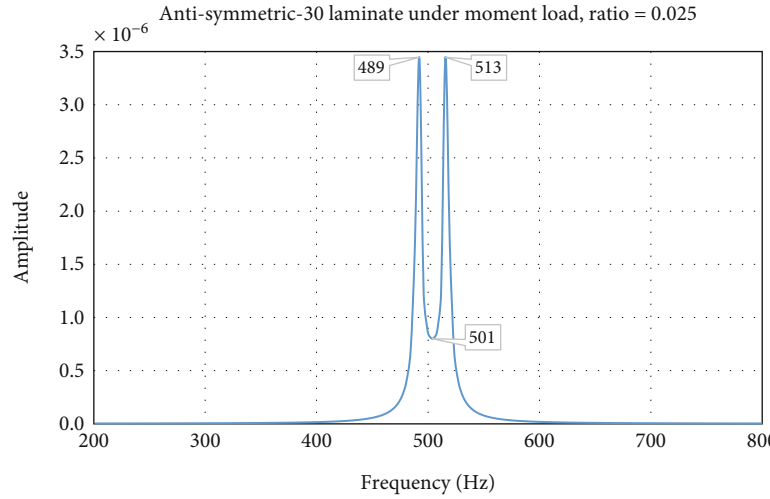
(c)

Figure 10: Continued.

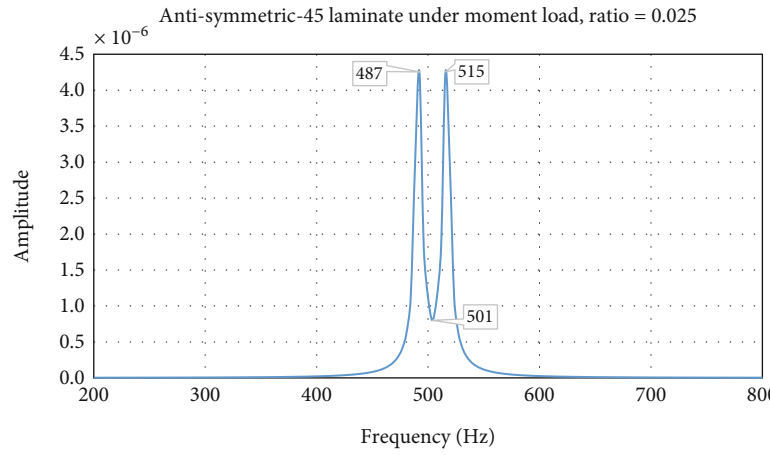
3962, 2026, 1, Downloaded from https://onlinelibrary.wiley.com/doi/10.1155/je/9725460 by Turkey Cochrane Evidence Aid, Wiley Online Library on [01/10/2026]. See the Terms and Conditions (https://onlinelibrary.wiley.com/terms-and-conditions) on Wiley Online Library for rules of use; OA articles are governed by the applicable Creative Commons License



(d)



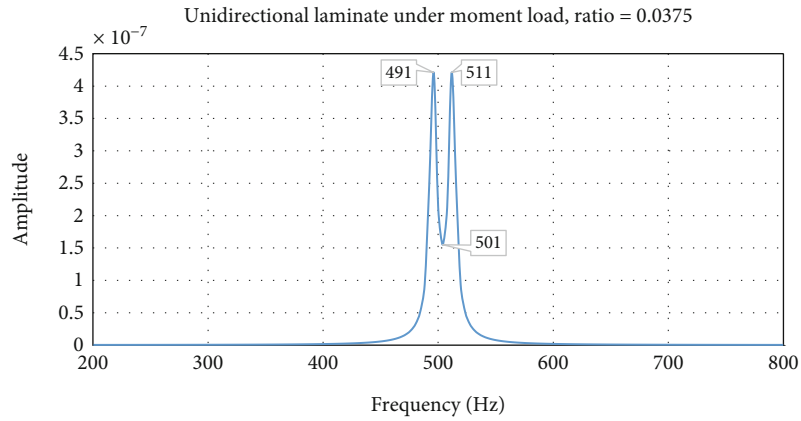
(e)



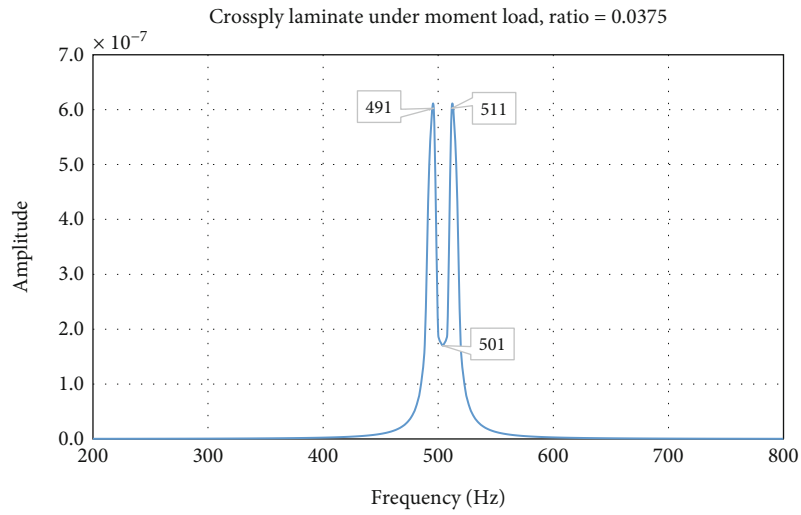
(f)

Figure 10: Fourier analysis of (a) unidirectional, (b) cross-ply, (c) symm-30, (d) symm-45, (e) anti-30, (f) anti-45 laminates under moment loading (ratio 0.025).

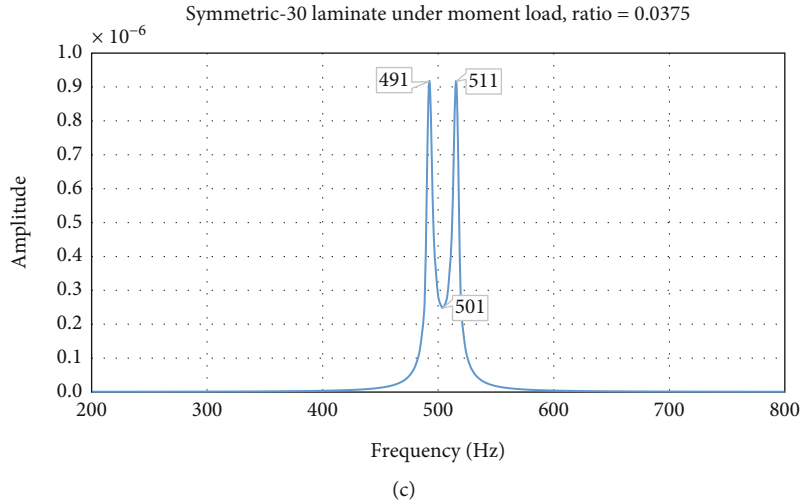
3962, 2026, 1, Downloaded from https://onlinelibrary.wiley.com/doi/10.1155/je/9725460 by Turkey Cochrane Evidence Aid, Wiley Online Library on [01/10/2026]. See the Terms and Conditions (https://onlinelibrary.wiley.com/terms-and-conditions) on Wiley Online Library for rules of use; OA articles are governed by the applicable Creative Commons License



(a)



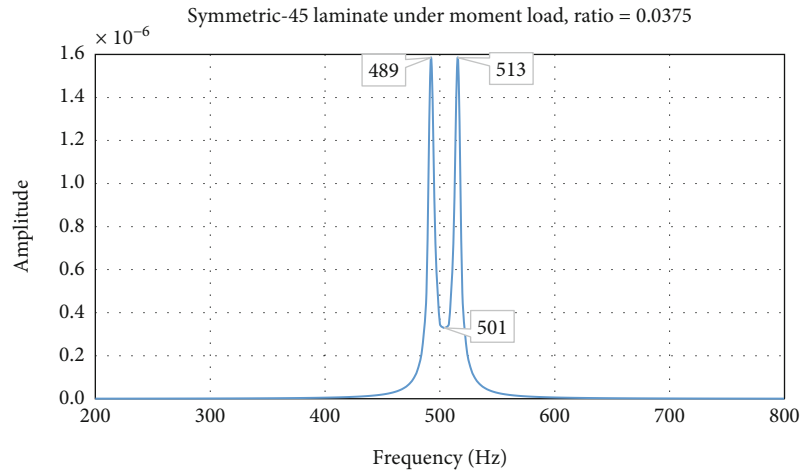
(b)



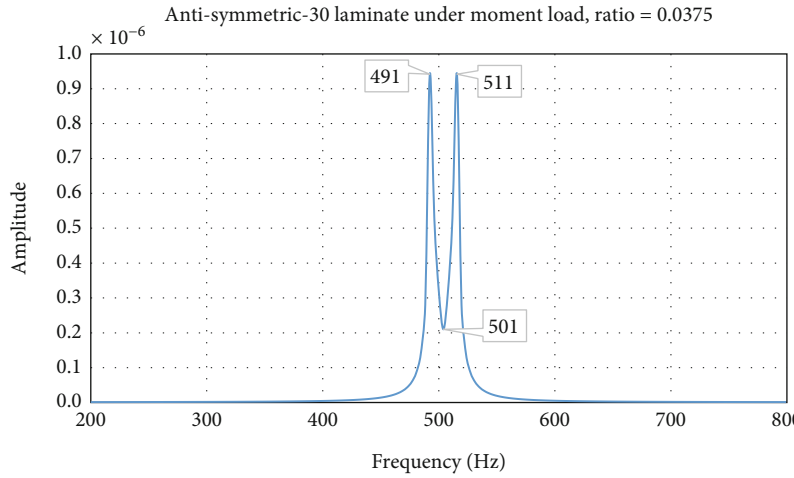
(c)

Figure 11: Continued.

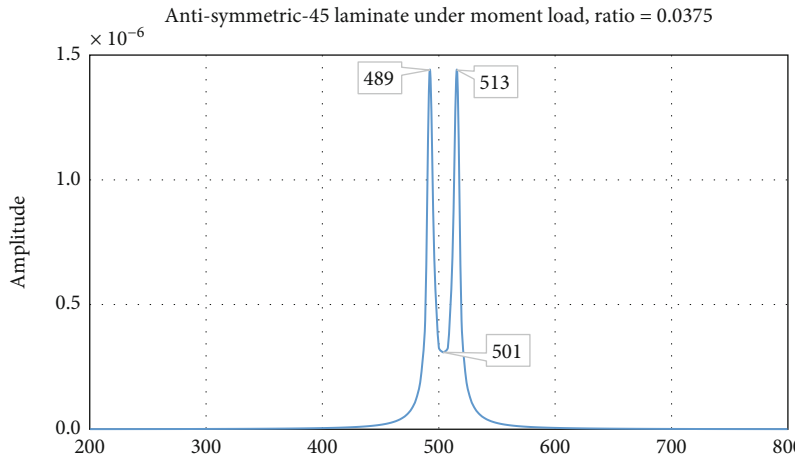
3962, 2026, 1, Downloaded from https://onlinelibrary.wiley.com/doi/10.1155/je/9725460 by Turkey Cochrane Evidence Aid, Wiley Online Library on [01/10/2026]. See the Terms and Conditions (https://onlinelibrary.wiley.com/terms-and-conditions) on Wiley Online Library for rules of use; OA articles are governed by the applicable Creative Commons License



(d)



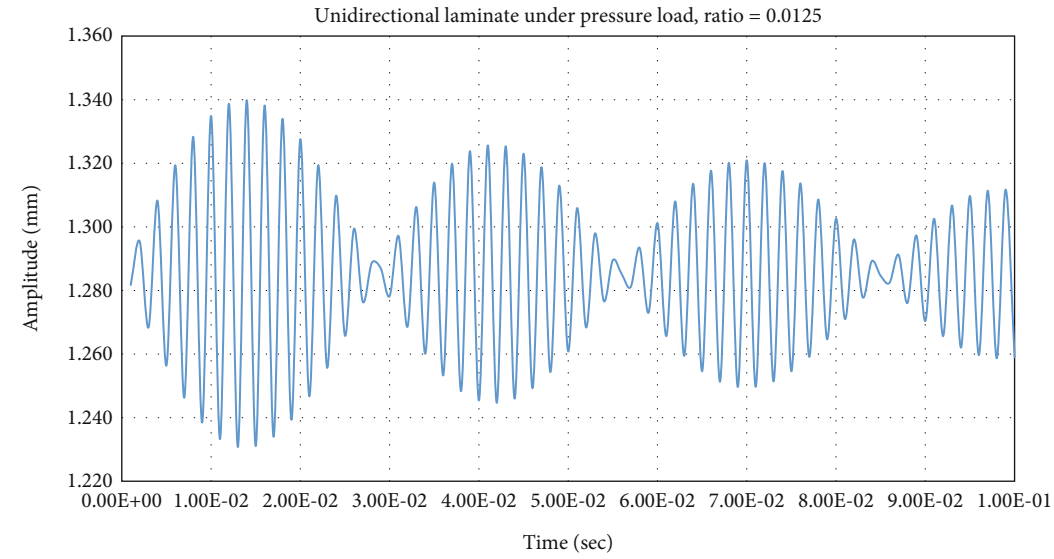
(e)



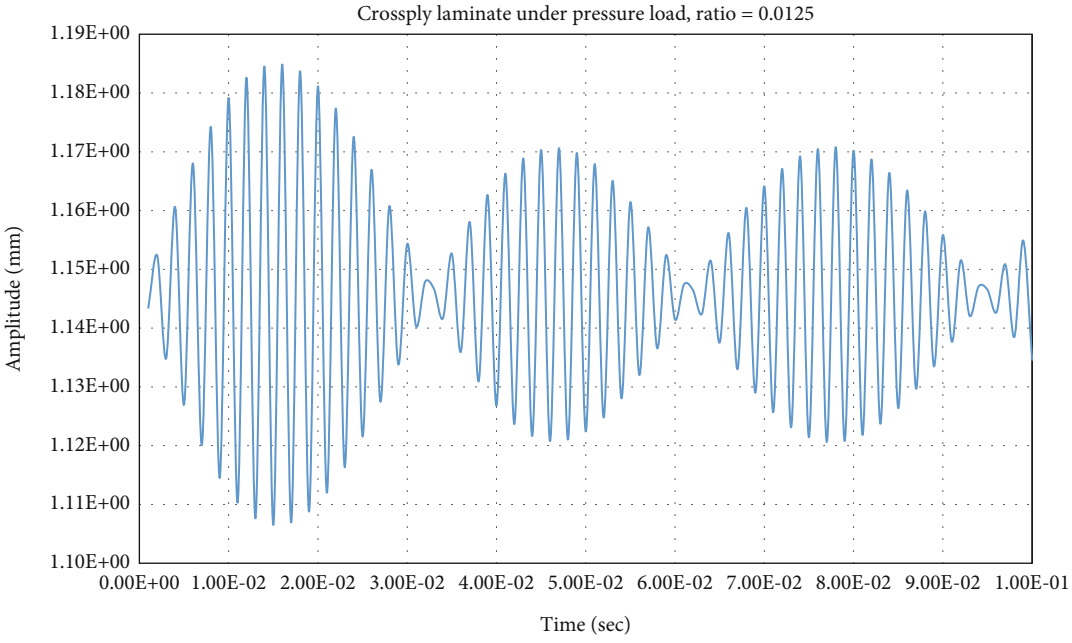
(f)

Figure 11: Fourier analysis of (a) unidirectional, (b) cross-ply, (c) symm-30, (d) symm-45, (e) anti-30, (f) anti-45 laminates under moment loading (ratio 0.0375).

3962, 2026, 1, Downloaded from https://onlinelibrary.wiley.com/doi/10.1155/je/9725460 by Turkey Cochrane Evidence Aid, Wiley Online Library on [01/10/2026]. See the Terms and Conditions (https://onlinelibrary.wiley.com/terms-and-conditions) on Wiley Online Library for rules of use; OA articles are governed by the applicable Creative Commons License



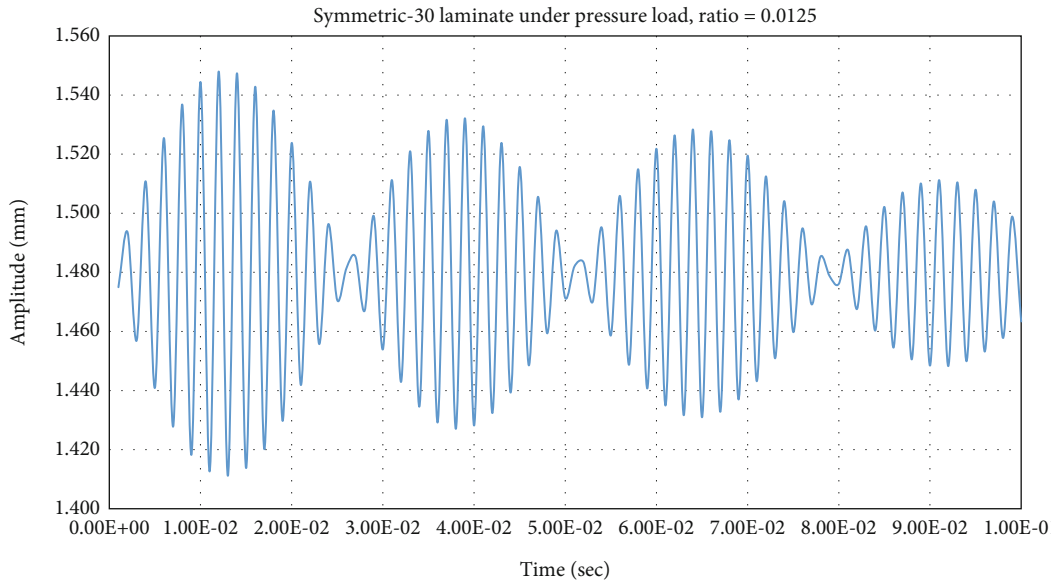
(a)



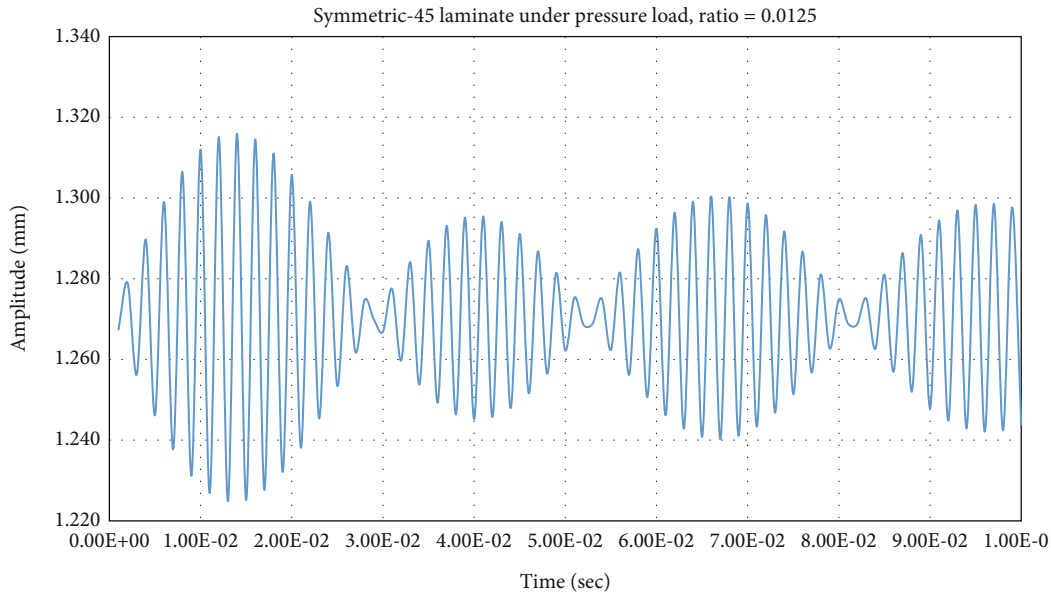
(b)

Figure 12: Continued.

3962, 2026, 1, Downloaded from https://onlinelibrary.wiley.com/doi/10.1155/je/9725460 by Turkey Cochrane Evidence Aid, Wiley Online Library on [01/10/2026]. See the Terms and Conditions (https://onlinelibrary.wiley.com/terms-and-conditions) on Wiley Online Library for rules of use; OA articles are governed by the applicable Creative Commons License



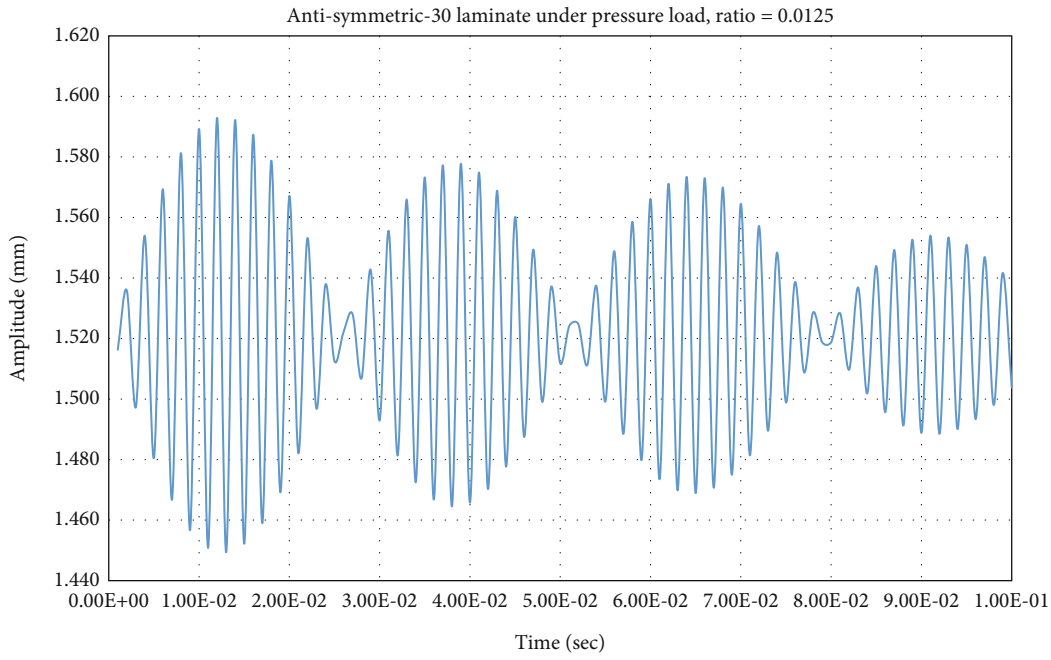
(c)



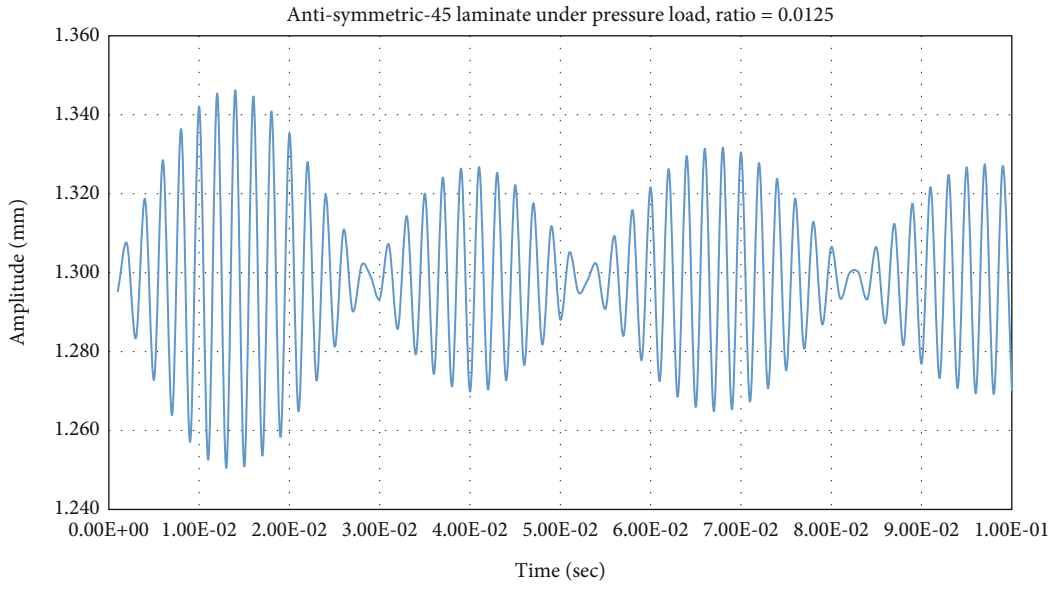
(d)

Figure 12: Continued.

3962, 2026, 1, Downloaded from https://onlinelibrary.wiley.com/doi/10.1155/je/9725460 by Turkey Cochrane Evidence Aid, Wiley Online Library on [01/10/2026]. See the Terms and Conditions (https://onlinelibrary.wiley.com/terms-and-conditions) on Wiley Online Library for rules of use; OA articles are governed by the applicable Creative Commons License



(e)



(f)

Figure 12: Dynamic response of (a) unidirectional, (b) cross-ply, (c) symm-30, (d) symm-45, (e) anti-30, (f) anti-45 laminates under pressure loading (ratio 0.0125).

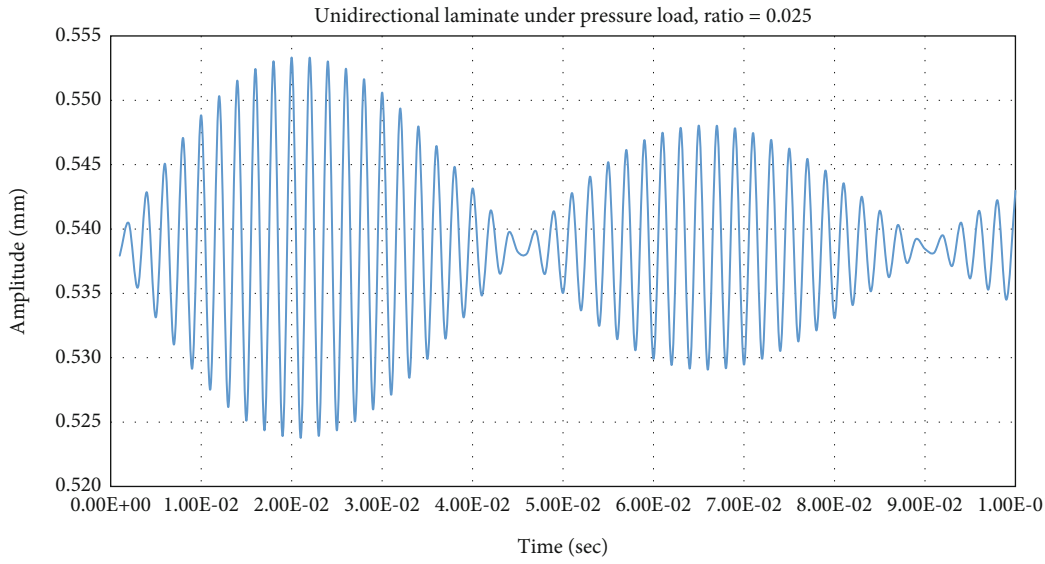
the natural frequency for this model. Figure 1 illustrates the structure and the associated boundary conditions.

2.2. Material Properties. The laminate consists of two materials, carbon prepreg and resin epoxy. The properties of the resulting lamina are calculated using ANSYS Material Designer and presented in Table 1.

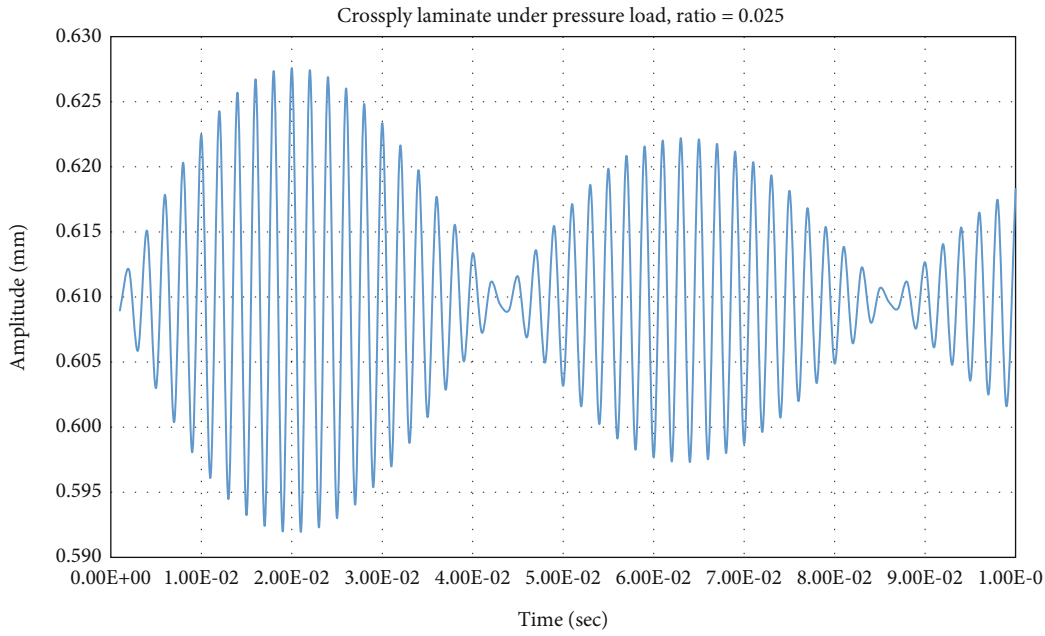
2.3. Stacking Sequence. All models consist of five layers with six different stacking sequences are considered in this investigation: unidirectional, cross-ply, symmetric-30, symmetric-45, anti-symmetric-30, and anti-symmetric-45. These stacking configurations represent distinct arrangement that influence the laminate's mechanical properties and response characteristics. The stiffness matrices corresponding to each staking sequence are provided in Table 2, and Figure 2 illustrates all stacking sequences.

2.4. Finite Element. Element SHELL181 was chosen in the analysis. It is a four-node structural element with total six degrees of freedom in the x, y, and z directions. The element formulation is based on the first-order shear deformation theory.

3962, 2026, 1, Downloaded from https://onlinelibrary.wiley.com/doi/10.1155/je/9725460 by Turkey Cochrane Evidence Aid, Wiley Online Library on [01/10/2026]. See the Terms and Conditions (https://onlinelibrary.wiley.com/terms-and-conditions) on Wiley Online Library for rules of use; OA articles are governed by the applicable Creative Commons License



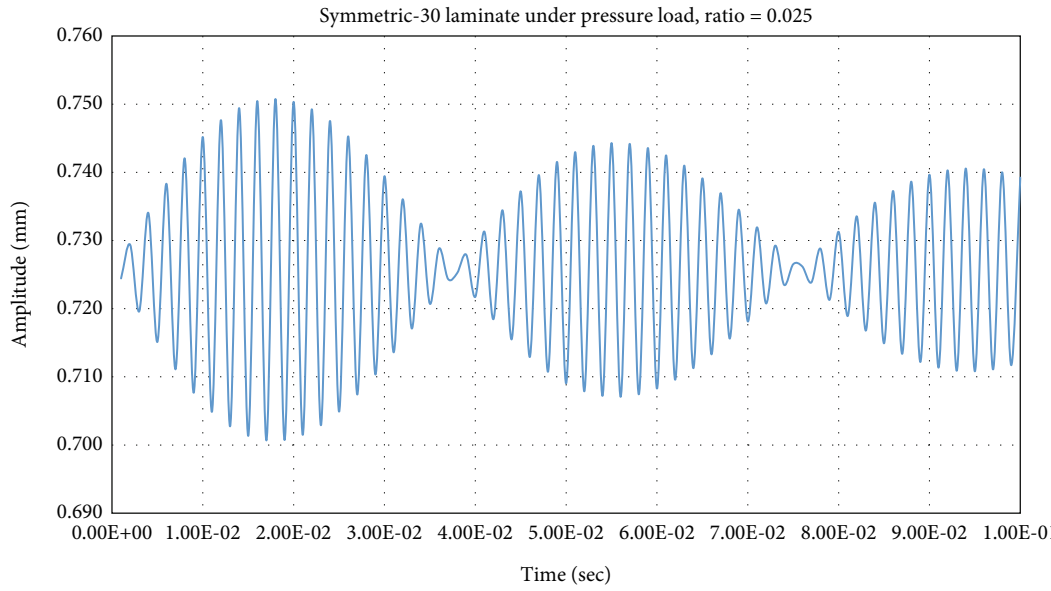
(a)



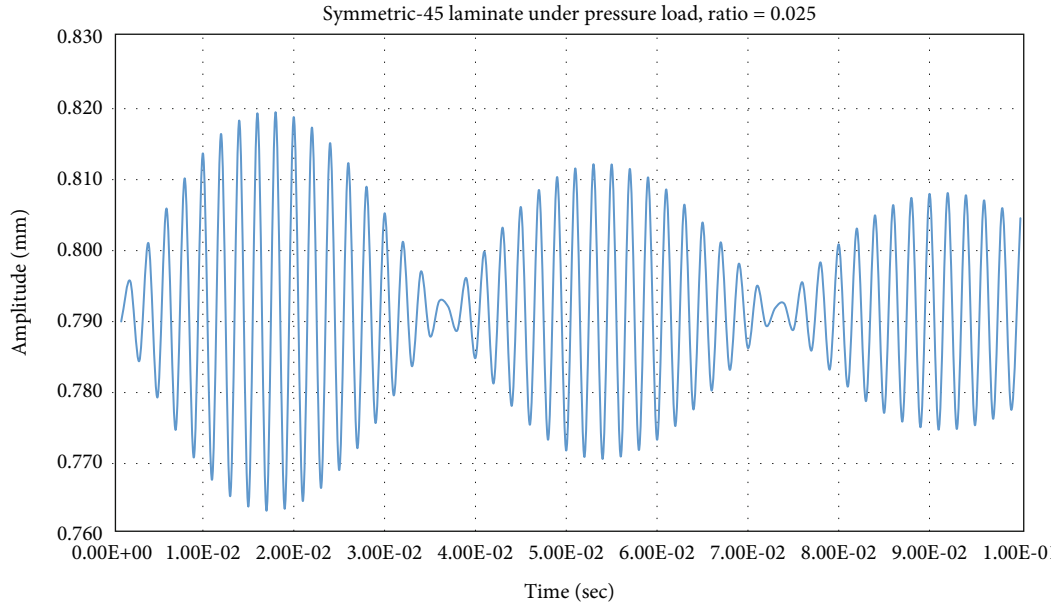
(b)

Figure 13: Continued.

3962, 2026, 1, Downloaded from https://onlinelibrary.wiley.com/doi/10.1155/je/9725460 by Turkey Cochrane Evidence Aid, Wiley Online Library on [01/10/2026]. See the Terms and Conditions (https://onlinelibrary.wiley.com/terms-and-conditions) on Wiley Online Library for rules of use; OA articles are governed by the applicable Creative Commons License



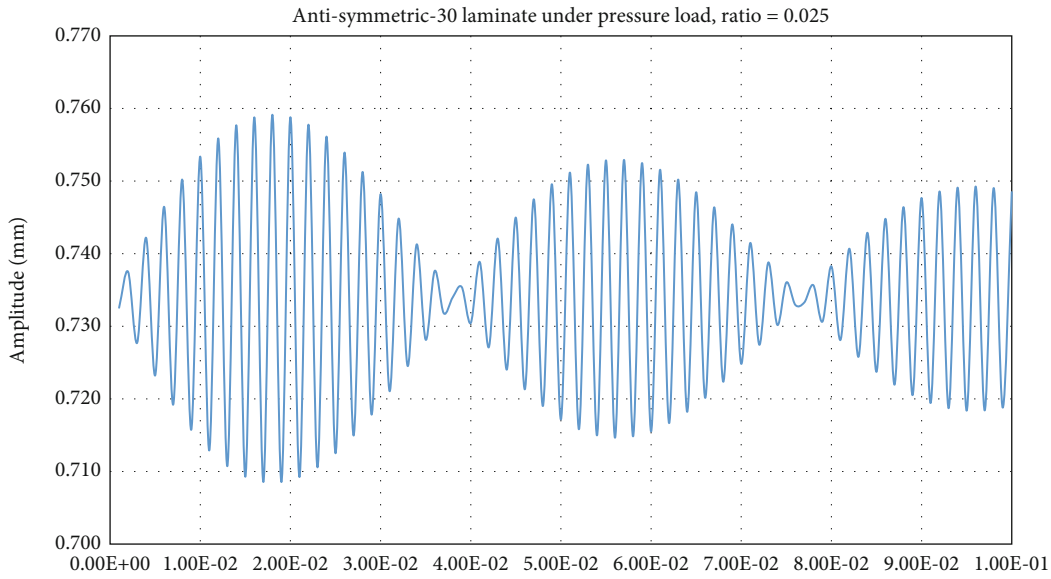
(c)



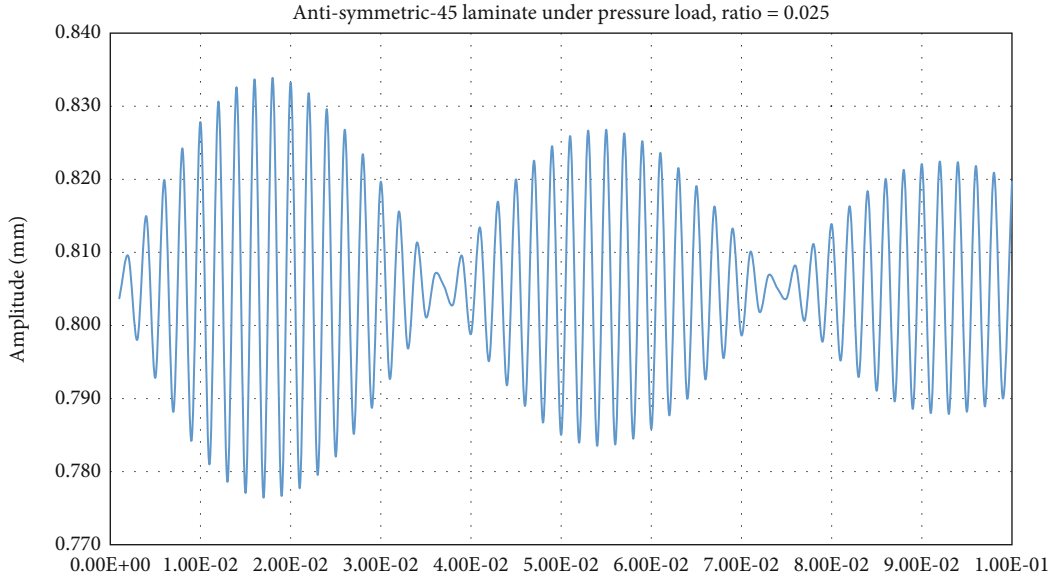
(d)

Figure 13: Continued.

3962, 2026, 1, Downloaded from https://onlinelibrary.wiley.com/doi/10.1155/je/9725460 by Turkey Cochrane Evidence Aid, Wiley Online Library on [01/10/2026]. See the Terms and Conditions (https://onlinelibrary.wiley.com/terms-and-conditions) on Wiley Online Library for rules of use; OA articles are governed by the applicable Creative Commons License



(e)



(f)

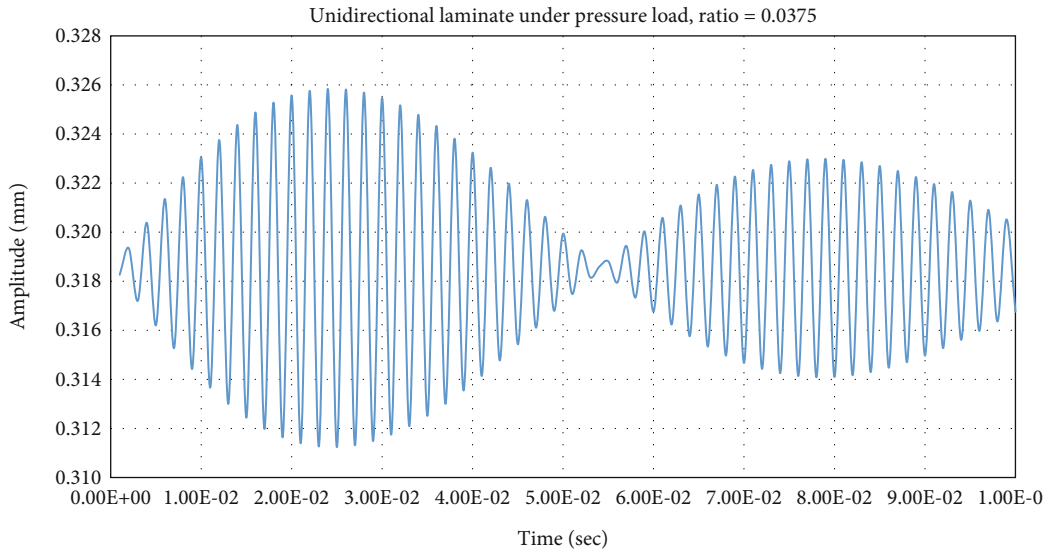
FIGURE 13: Dynamic response of (a) unidirectional, (b) cross-ply, (c) symm-30, (d) symm-45, (e) anti-30, (f) anti-45 laminates under pressure loading (ratio 0.025).

The laminated composite is discretized and meshed using quadrilateral shell elements. The discretization is done such that all elements are square-shaped and have the same size, thus avoiding any skewness or deficiencies in the elements.

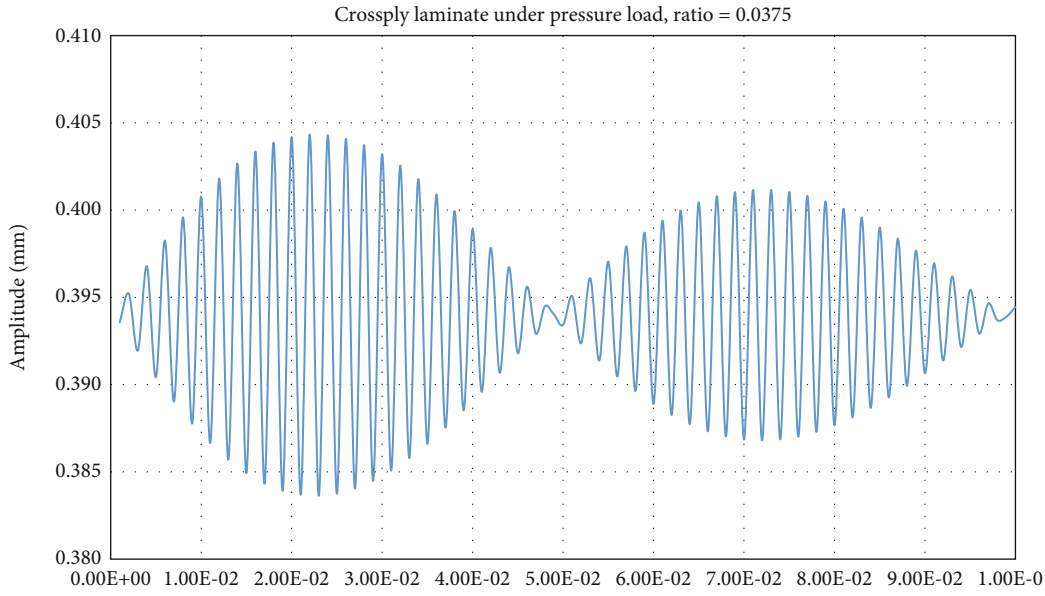
As stated earlier, all models are simply supported on all edges. Two different types of step loading are considered in the study, pressure and moment. These loads are applied as a step function and maintained throughout the analysis duration as shown in Figure 3.

2.4.1. Finite Element Model. The mesh was determined and validated through a convergence study. The study utilized models under moment loading with thickness/length of 0.0125. Table 3 represents the values of the mid-node deflection analysis under various element sizes; the last column represents the error percentage between the deflection values obtained from the last two smallest mesh sizes. As can be noted, the error is very small, implying that the 100×100 mesh produces precise results with maximum relative difference less than 3%. Clearly, the results affirm that the chosen

3962, 2026, 1, Downloaded from https://onlinelibrary.wiley.com/doi/10.1155/je/9725460 by Turkey Cochrane Evidence Aid, Wiley Online Library on [01/10/2026]. See the Terms and Conditions (https://onlinelibrary.wiley.com/terms-and-conditions) on Wiley Online Library for rules of use; OA articles are governed by the applicable Creative Commons License



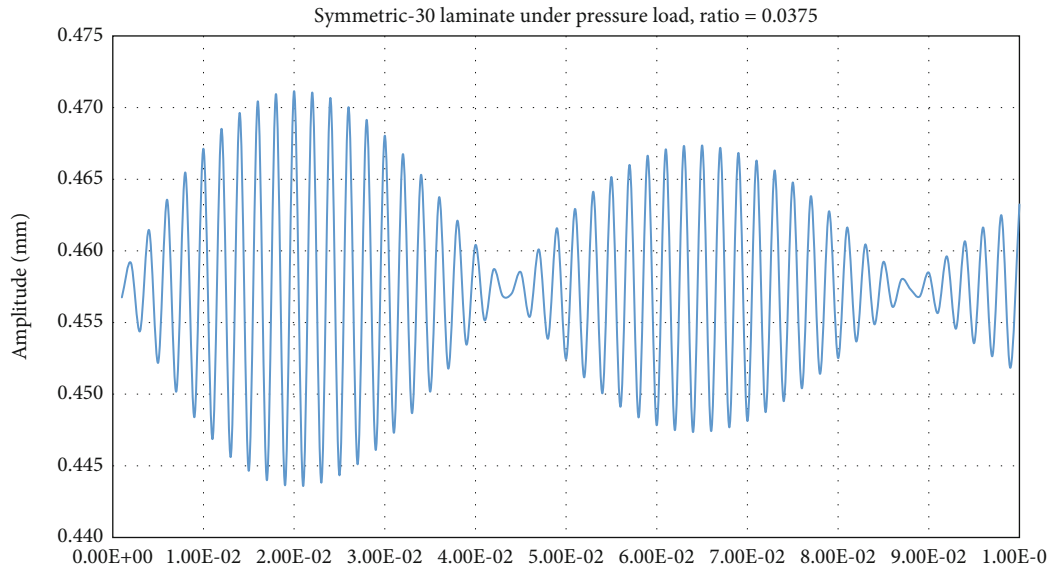
(a)



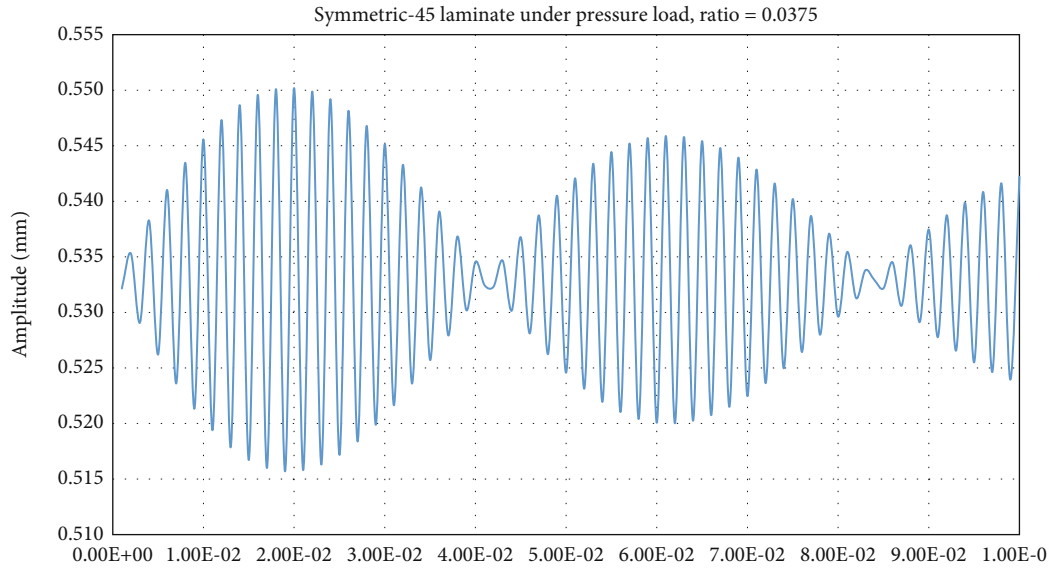
(b)

Figure 14: Continued.

3962, 2026, 1, Downloaded from https://onlinelibrary.wiley.com/doi/10.1155/je/9725460 by Turkey Cochrane Evidence Aid, Wiley Online Library on [01/10/2026]. See the Terms and Conditions (https://onlinelibrary.wiley.com/terms-and-conditions) on Wiley Online Library for rules of use; OA articles are governed by the applicable Creative Commons License



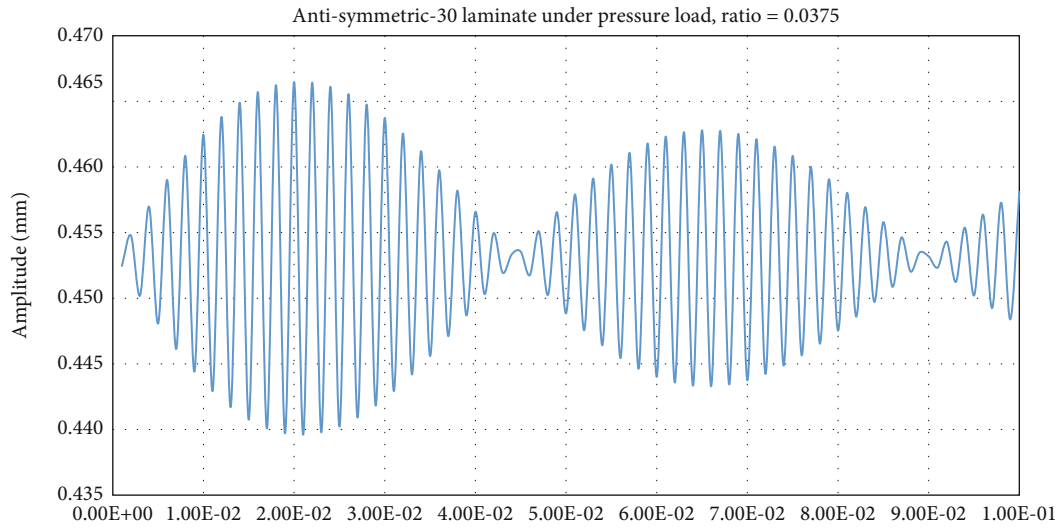
(c)



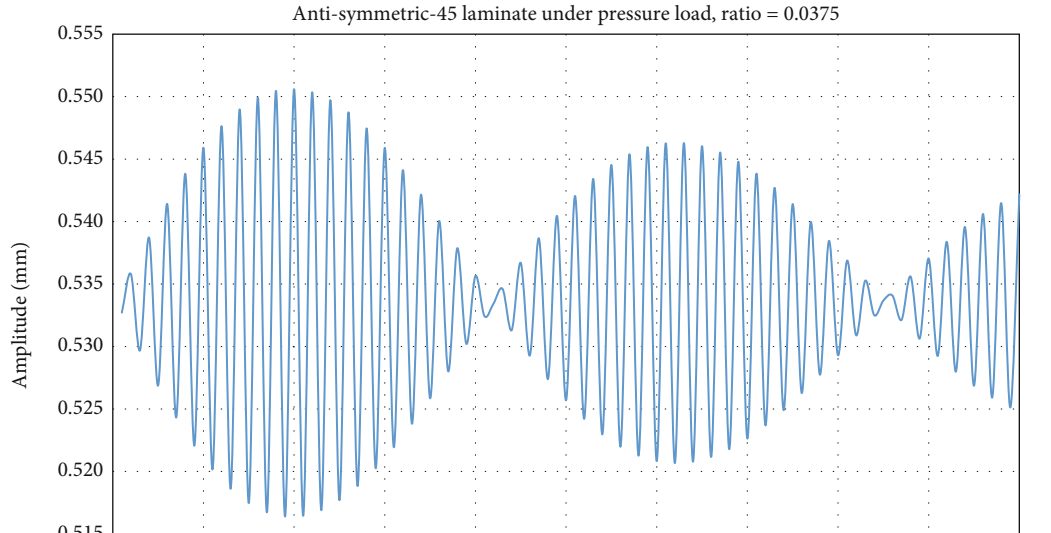
(d)

Figure 14: Continued.

3962, 2026, 1, Downloaded from https://onlinelibrary.wiley.com/doi/10.1155/je/9725460 by Turkey Cochrane Evidence Aid, Wiley Online Library on [01/10/2026]. See the Terms and Conditions (https://onlinelibrary.wiley.com/terms-and-conditions) on Wiley Online Library for rules of use; OA articles are governed by the applicable Creative Commons License



(e)



(f)

Figure 14: Dynamic response of (a) unidirectional, (b) cross-ply, (c) symm-30, (d) symm-45, (e) anti-30, (f) anti-45 laminates under pressure loading (ratio 0.0375).

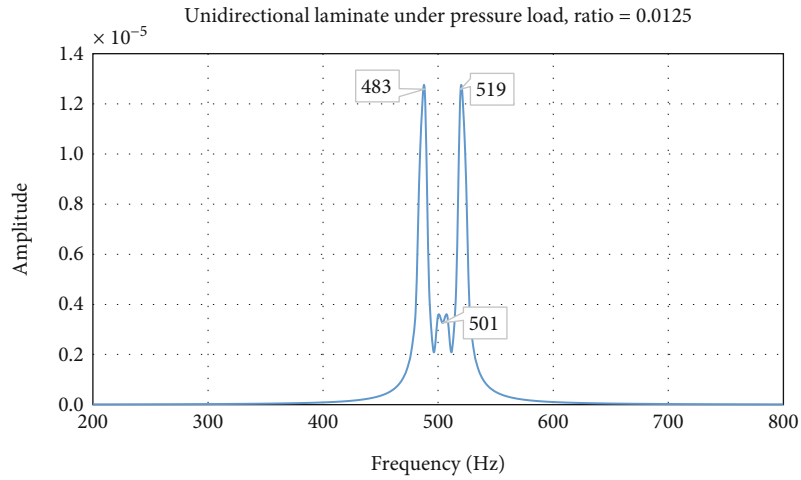
100×100 mesh size does comprise solution convergence. Figure 4 shows the finite model.

2.4.2. Finite Model Validation. To ensure the reliability of the finite model employed in the study, the model was tested against analytical solutions. Since no experimental validation was performed, the verification was carried out by comparing the numerical predictions with the established analytical results from the literature.

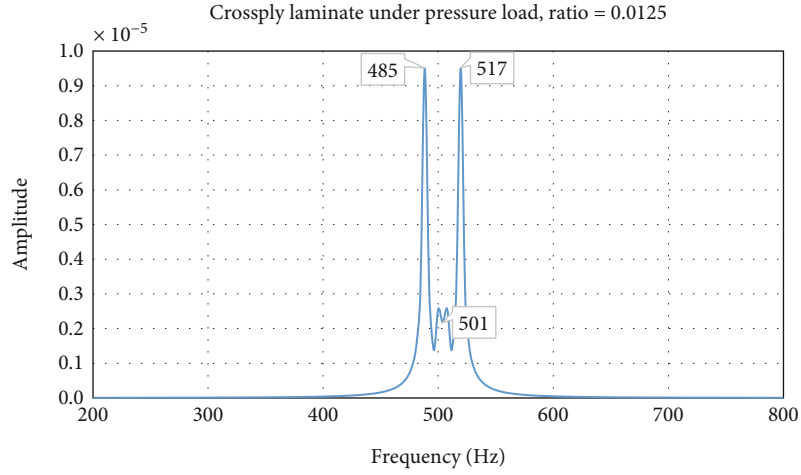
Several studies have relied on analytical solutions to verify their computational models. Swaddiwudhipong et al. [30], for example, analyzed laminated composite plates using modified degenerate shell elements, and their results demonstrated good agreement with those reported by Kant et al. [5]. The latter study also confirmed consistency with the analytical solutions presented by Reddy [1]. Thus, both studies can be utilized as a benchmark for validating finite models. Referring to example 1—a simply supported anisotropic square plate—reported by Swaddiwudhipong et al. [30], this example served as a comparative reference in this work.

The same material, stacking, loading, and boundary conditions were replicated using our finite element model. The results obtained are compared with the results from the reference example, and are presented in Figure 5. As noted

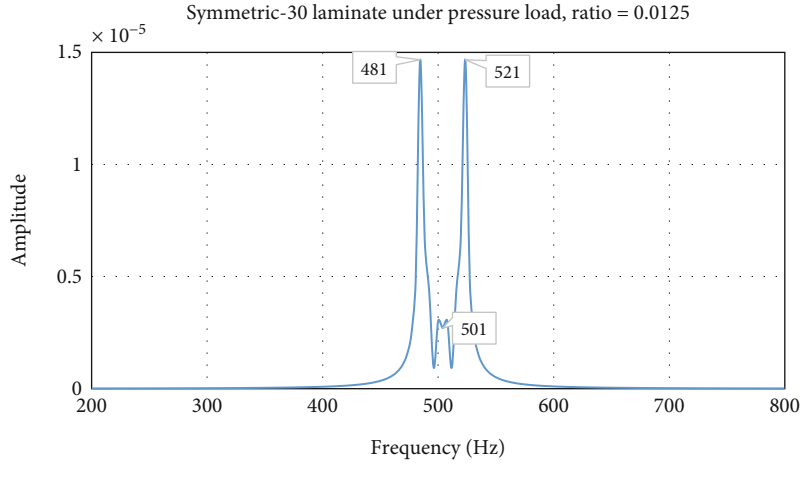
3962, 2026, 1, Downloaded from https://onlinelibrary.wiley.com/doi/10.1155/je/9725460 by Turkey Cochrane Evidence Aid, Wiley Online Library on [01/10/2026]. See the Terms and Conditions (https://onlinelibrary.wiley.com/terms-and-conditions) on Wiley Online Library for rules of use; OA articles are governed by the applicable Creative Commons License



(a)



(b)



(c)

Figure 15: Continued.

3962, 2026, 1, Downloaded from https://onlinelibrary.wiley.com/doi/10.1155/je/9725460 by Turkey Cochrane Evidence Aid, Wiley Online Library on [01/10/2026]. See the Terms and Conditions (https://onlinelibrary.wiley.com/terms-and-conditions) on Wiley Online Library for rules of use; OA articles are governed by the applicable Creative Commons License

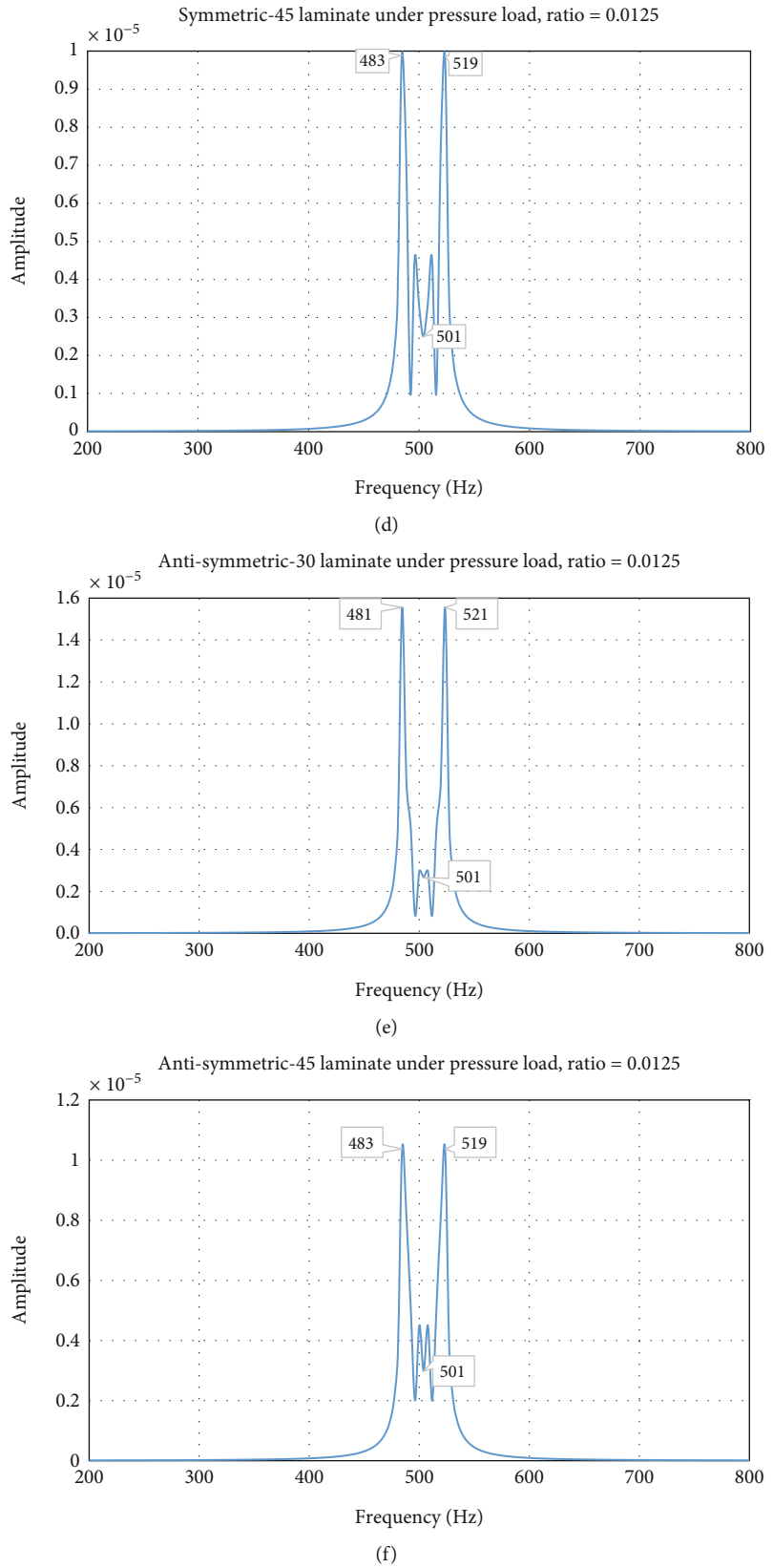
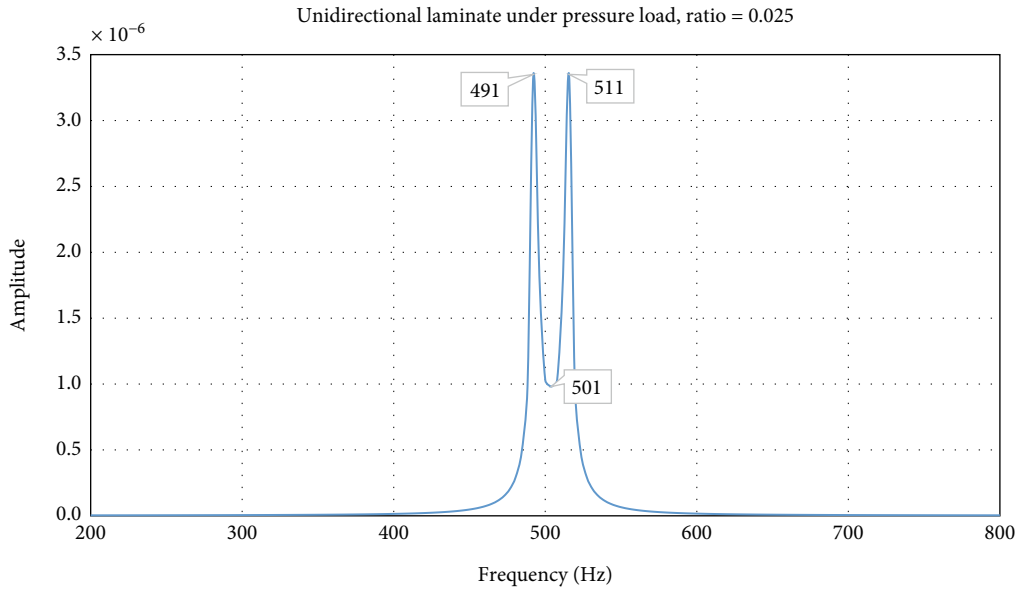
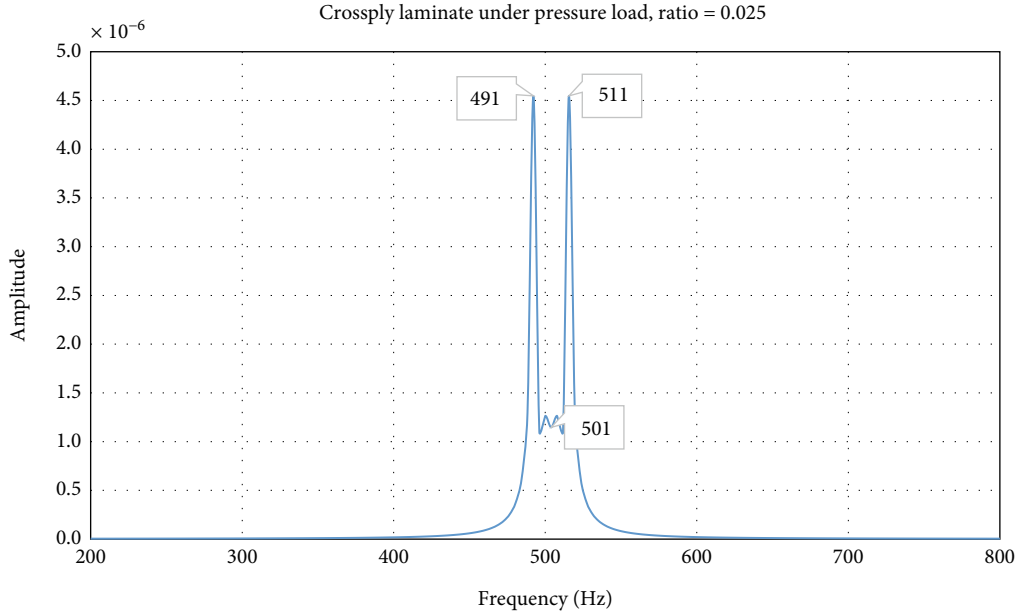


Figure 15: Fourier analysis of (a) unidirectional, (b) cross-ply, (c) symm-30, (d) symm-45, (e) anti-30, (f) anti-45 laminates under pressure loading (ratio 0.0125).

3962, 2026, 1, Downloaded from https://onlinelibrary.wiley.com/doi/10.1155/je/9725460 by Turkey Cochrane Evidence Aid, Wiley Online Library on [01/10/2026]. See the Terms and Conditions (https://onlinelibrary.wiley.com/terms-and-conditions) on Wiley Online Library for rules of use; OA articles are governed by the applicable Creative Commons License



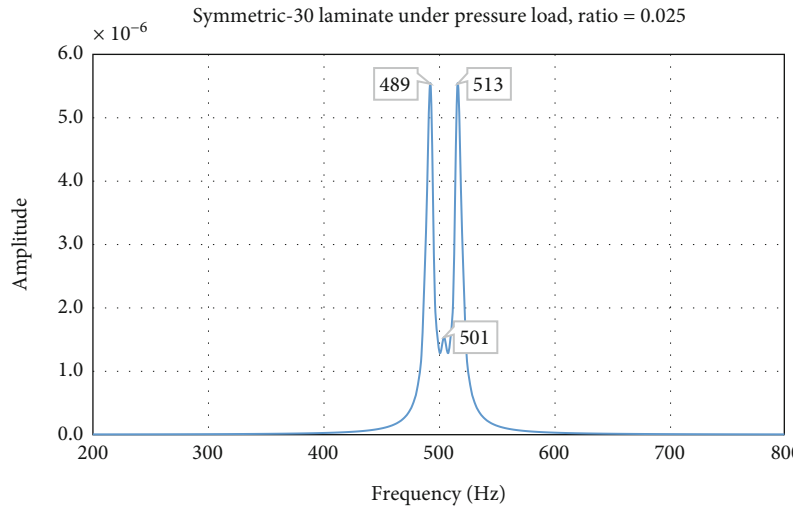
(a)



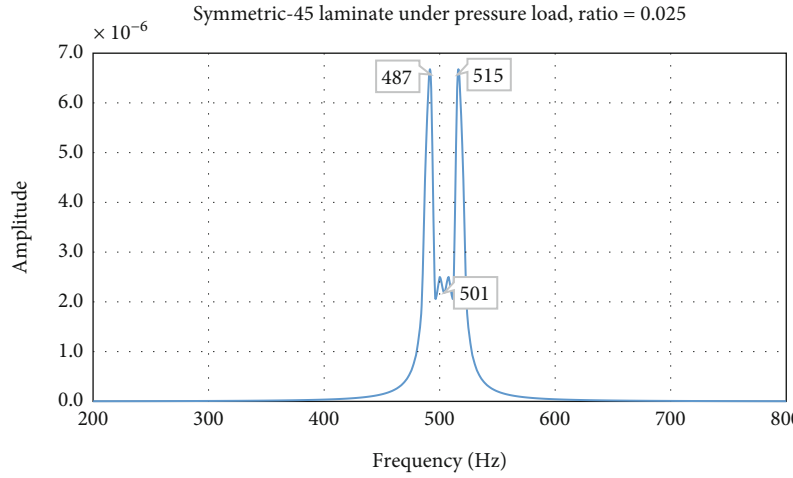
(b)

Figure 16: Continued.

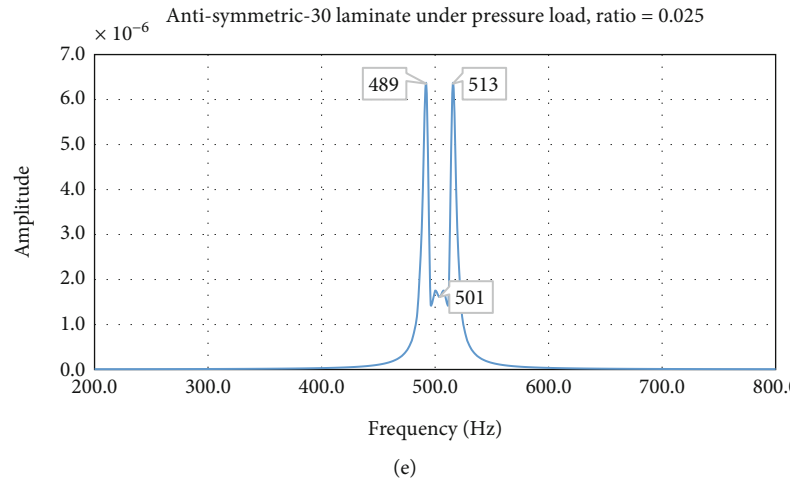
3962, 2026, 1, Downloaded from https://onlinelibrary.wiley.com/doi/10.1155/je/9725460 by Turkey Cochrane Evidence Aid, Wiley Online Library on [01/10/2026]. See the Terms and Conditions (https://onlinelibrary.wiley.com/terms-and-conditions) on Wiley Online Library for rules of use; OA articles are governed by the applicable Creative Commons License



(c)



(d)



(e)

Figure 16: Continued.

3962, 2026, 1, Downloaded from https://onlinelibrary.wiley.com/doi/10.1155/je/9725460 by Turkey Cochrane Evidence Aid, Wiley Online Library on [01/10/2026]. See the Terms and Conditions (https://onlinelibrary.wiley.com/terms-and-conditions) on Wiley Online Library for rules of use; OA articles are governed by the applicable Creative Commons License

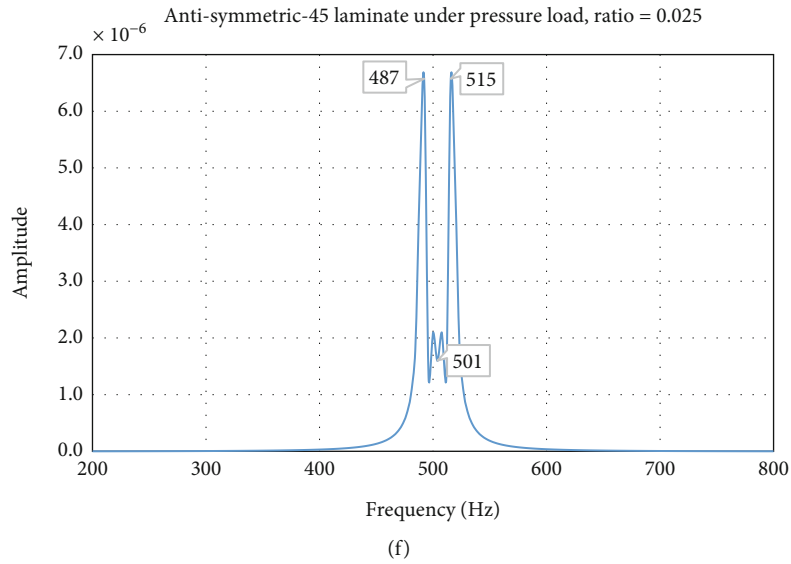


Figure 16: Fourier analysis of (a) unidirectional, (b) cross-ply, (c) symm-30, (d) symm-45, (e) anti-30, (f) anti-45 laminates under pressure loading (ratio 0.025).

from the figure, the present solution exhibits excellent agreement with the benchmark solution with relative error below 5%. This consistency confirms that the developed finite element model is capable of accurately capturing the structural response of laminated composite plates under transient loading, thereby validating the correctness and robustness of the present model.

3. Results and Discussion

The investigation of the dynamic response of composite plate considered six different stacking sequences, three thickness to length ratios and two types of applied loads, resulting in 36 models. These models are summarized in Table 4, which provides a comprehensive overview of all configurations.

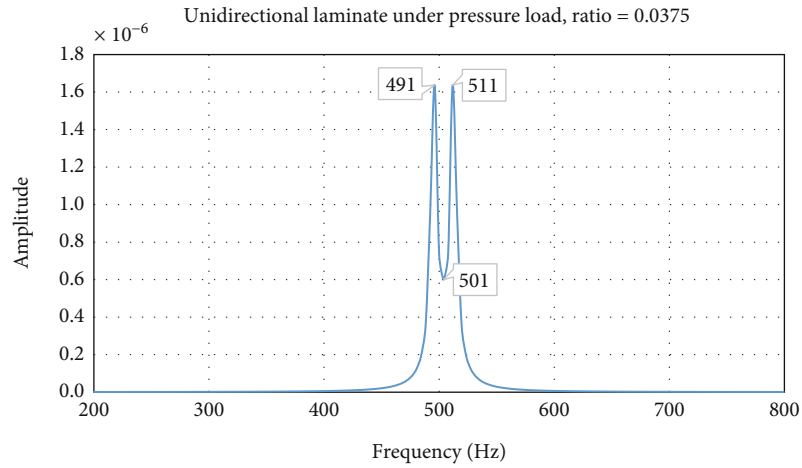
3.1. Cases Under Moment Loading. Figures 6, 7, and 8 show the dynamic responses of all laminates under moment loading. The results were obtained through numerical simulation using ANSYS software.

The responses offer insight into the structure behavior under moment loading conditions. In conjunction with the dynamic responses, Table 5 represents detailed data about the amplitude characteristics of each model. This table provides quantitative information about the quasi-static and maximum deformation amplitude experienced by different stacking sequences and thickness to length ratios. Additionally, Figures 9, 10, and 11 shows the frequency characteristics of the responses through frequency domain analysis, employing Fourier transform through MATLAB software.

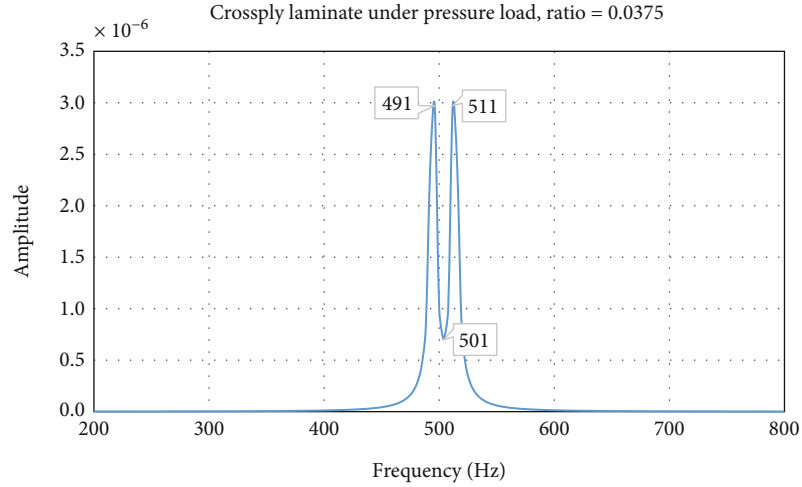
Figure 6 depicts the response of all laminates with thickness to length ratio of 0.0125. It is noted that despite differences in stacking sequence, the behavior of all laminates' responses remains consistent, as a qualitative pattern. This observation can be extended to laminates with thickness to length ratio of 0.025 and 0.0375. Figures 6, 7, and 8 provide visual conformation of this observation by illustrating that all laminates' responses exhibit similar displacement profile and frequency characteristics. Also, it is noted that all responses exhibit a single frequency, and it is nearly the same value, as indicated by Figures 9, 10, and 11. However, there are variations in amplitude characteristics among different stacking sequences. Table 5 provides data on the average and maximum amplitude values for each model. Correlating with Figure 6, which shows laminates with a thickness to length ratio of 0.0125, it is observed that the cross-ply laminate exhibits the smallest deformation amplitudes, followed by the unidirectional laminate. The symmetric-30 and anti-symmetric-30 laminates show the highest deformation, with the symmetric-45 and the anti-symmetric-45 falling in the middle. By further analyzing, it is observed that the symmetric-30 and anti-symmetric-30 exhibit the widest range of vibration motion, i.e., peak to trough, followed by the symmetric-45 and symmetric-45. Whereas the cross-ply laminate exhibits the smallest range of vibration motion.

Upon increasing thickness of the laminate, some observations made for laminates with thickness to length ratio of 0.0125 can be extended to those of ratios of 0.025 and 0.0375. In all cases, the displacement profile remained consistent, and the response consists of a single frequency. However, with respect to laminates with thickness to length ratio of 0.025, although the cross-ply laminate still exhibits the smallest deformation, it is the symmetric-45 and anti-symmetric-45 laminates that has the largest deformation amplitudes. As for the laminates with a thickness to length ratio of 0.0375, the unidirectional laminate exhibits the smallest deformation amplitudes and vibration motion. Also, the symmetric-45 and anti-symmetric-45 still has the largest deformation. However, the symmetric laminates have higher deformation amplitude than their anti-symmetric counterparts.

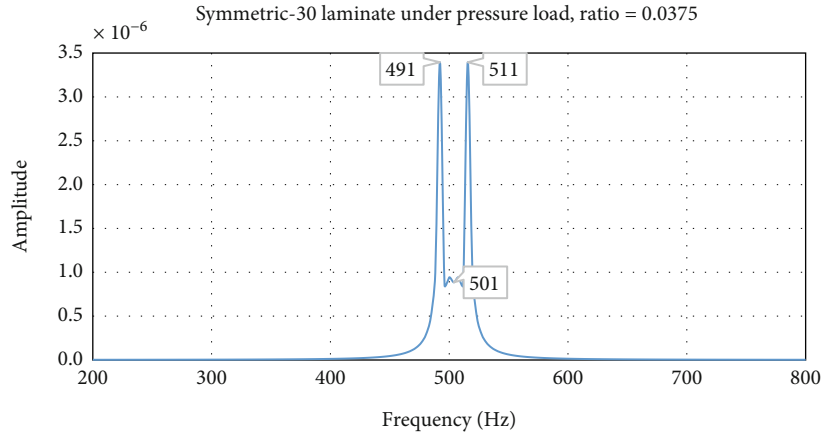
3962, 2026, 1, Downloaded from https://onlinelibrary.wiley.com/doi/10.1155/je/9725460 by Turkey Cochrane Evidence Aid, Wiley Online Library on [01/10/2026]. See the Terms and Conditions (https://onlinelibrary.wiley.com/terms-and-conditions) on Wiley Online Library for rules of use; OA articles are governed by the applicable Creative Commons License



(a)



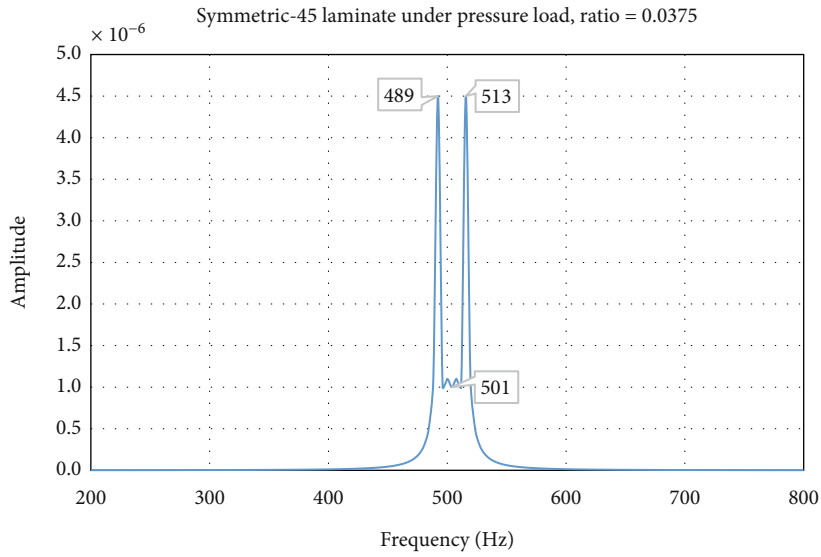
(b)



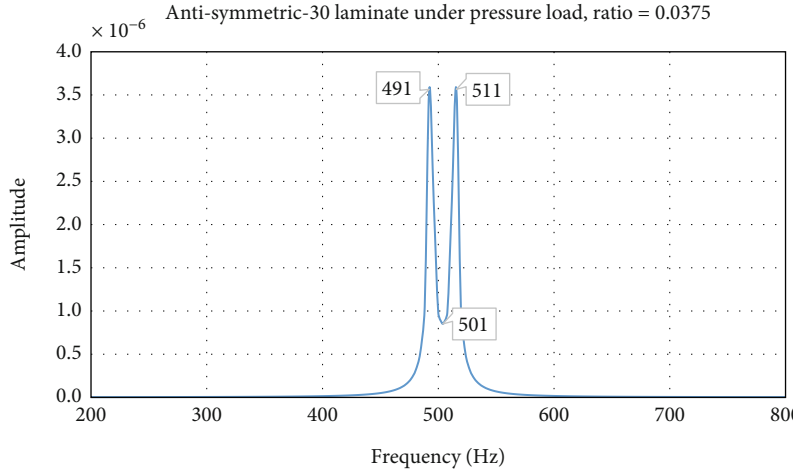
(c)

Figure 17: Continued.

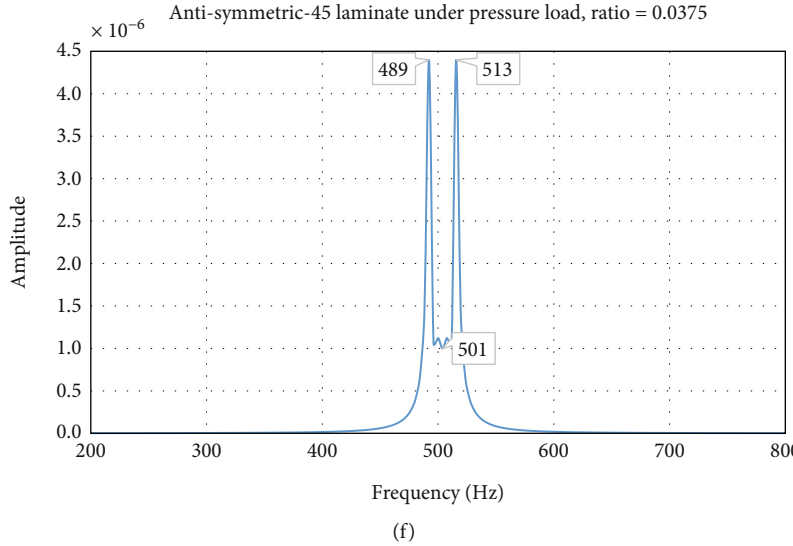
3962, 2026, 1, Downloaded from https://onlinelibrary.wiley.com/doi/10.1155/je/9725460 by Turkey Cochrane Evidence Aid, Wiley Online Library on [01/10/2026]. See the Terms and Conditions (https://onlinelibrary.wiley.com/terms-and-conditions) on Wiley Online Library for rules of use; OA articles are governed by the applicable Creative Commons License



(d)



(e)



(f)

Figure 17: Fourier analysis of (a) unidirectional, (b) cross-ply, (c) symm-30, (d) symm-45, (e) anti-30, (f) anti-45 laminates under pressure loading (ratio 0.0375).

3962, 2026, 1, Downloaded from https://onlinelibrary.wiley.com/doi/10.1155/je/9725460 by Turkey Cochrane Evidence Aid, Wiley Online Library on [01/10/2026]. See the Terms and Conditions (https://onlinelibrary.wiley.com/terms-and-conditions) on Wiley Online Library for rules of use; OA articles are governed by the applicable Creative Commons License

TABLE 6: Summary results of average and maximum displacement of laminates under pressure load, ratios 0.0125, 0.025, and 0.0375.

Stacking	Thickness/length	Average/thickness	Maximum/thickness	Deformation range (mm)
Unidirectional	0.0125	1.016	1.052	0.109
Cross-ply	0.0125	0.917	0.948	0.0783
Symmetric-30	0.0125	1.184	1.238	0.137
Symmetric-45	0.0125	1.028	1.071	0.0911
Anti-symmetric-30	0.0125	1.217	1.274	0.144
Anti-symmetric-45	0.0125	1.039	1.077	0.0957
Unidirectional	0.025	0.244	0.251	0.0296
Cross-ply	0.025	0.215	0.221	0.0356
Symmetric-30	0.025	0.290	0.300	0.0501
Symmetric-45	0.025	0.317	0.328	0.0561
Anti-symmetric-30	0.025	0.294	0.304	0.0506
Anti-symmetric-45	0.025	0.322	0.334	0.0574
Unidirectional	0.0375	0.0994	0.0998	0.146
Cross-ply	0.0375	0.101	0.104	0.207
Symmetric-30	0.0375	0.121	0.124	0.276
Symmetric-45	0.0375	0.142	0.144	0.345
Anti-symmetric-30	0.0375	0.122	0.126	0.268
Anti-symmetric-45	0.0375	0.142	0.147	0.342

TABLE 7: Modal data for fiber material.

Model type	Thickness/ length	Thickness (mm)	Frequency (Hz)
Lamina	0.0125	0.25	17.05
Trans. section	0.0125	0.977613	135.34
Laminate	0.0125	1.25	195.68
Lamina	0.025	0.5	49.505
Trans. section	0.025	1.95528	382.83
Laminate	0.025	2.5	553.489
Lamina	0.0375	0.075	90.95
Trans. section	0.0375	2.932	702.98
Laminate	0.0375	3.75	1016.8

TABLE 8: Modal data for epoxy material.

Model type	Thickness/ length	Thickness (mm)	Frequency (Hz)
Lamina	0.0125	0.25	4.263
Trans. section	0.0125	10.216	1113.7
Laminate	0.0125	1.25	47.66
Lamina	0.025	0.5	12.06
Trans. section	0.025	20.432	3158.7
Laminate	0.025	2.5	134.81
Lamina	0.0375	0.75	22.152
Trans. section	0.0375	30.648	5784.5
Laminate	0.0375	3.75	247.67

A comparative analysis of the stiffness matrices for laminates with thickness to length ratio of 0.0125 reveals that for any of the anti-symmetric laminates and its counterpart, the extensional matrix is the same. However, the difference arises in the elements D_{16} and D_{26}, which makes the symmetric laminates stronger in resisting bending on the x and y axes. The closeness of the results between the symmetric and its counterpart is attributed to the B_{16} and B_{26} in the anti-symmetric laminates. As for the unidirectional and cross-ply laminates, their small deformation is attributed to their high stiffness along either/or both the x and y axes. The laminate possesses strong resistance to bending due to the high tension induced.

Regarding laminates with thickness to length ratio of 0.025, the marginal differences in the deformation values persist between the symmetric laminates and their counterparts, as well as the unidirectional and cross-ply laminates. These discrepancies are attributed to the same factors explained for laminates with thickness to length ratio of 0.0125. The difference arises in the symmetric-45 and anti-symmetric-45 laminates exhibiting higher deformation than the symmetric-30 and anti-symmetric-30, respectively. The reason is that despite some elements in stiffness matrix of symmetric-45 and anti-symmetric-45 that possess higher values compared to their symmetric-30 and anti-symmetric-30, it is noteworthy that these elements resist shear deformation rather than bending. However, elements A_{11},

3962, 2026, 1, Downloaded from https://onlinelibrary.wiley.com/doi/10.1155/je/9725460 by Turkey Cochrane Evidence Aid, Wiley Online Library on [01/10/2026]. See the Terms and Conditions (https://onlinelibrary.wiley.com/terms-and-conditions) on Wiley Online Library for rules of use; OA articles are governed by the applicable Creative Commons License

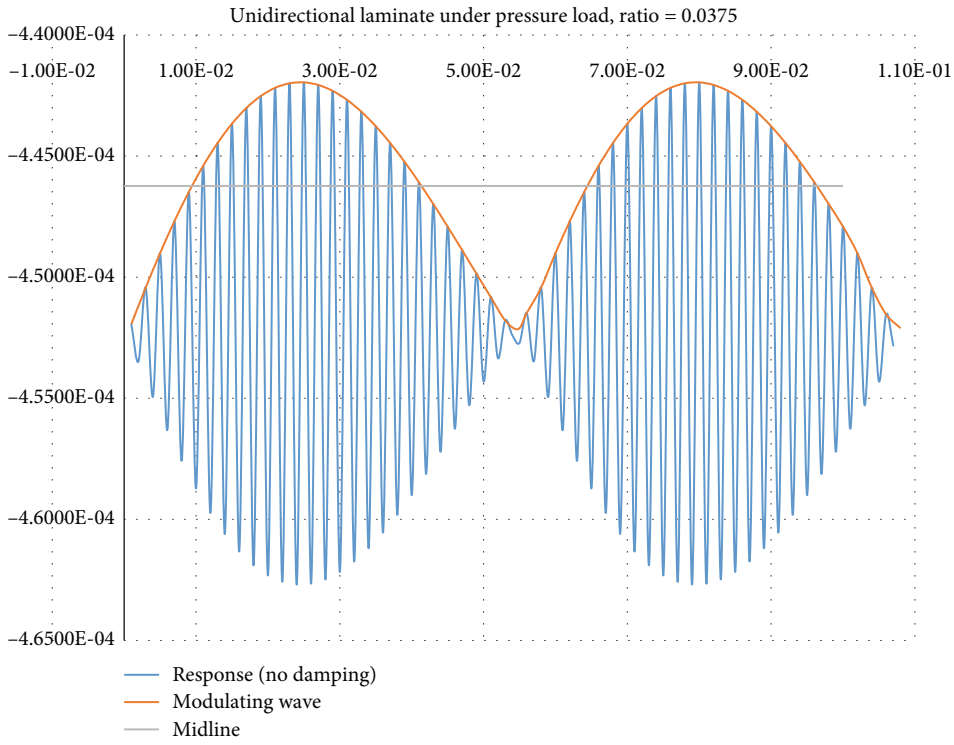


Figure 18: Undamped response of unidirectional laminate under pressure load, ratio 0.0375.

B_{16}, and D_{11}, which provide better contribution to bending, has higher values for symmetric-30 and anti-symmetric-30 laminates.

For laminates with thickness to length ratio of 0.0375, the unidirectional laminate exhibits the smallest deformation due to its significant resistance to tension compared to other laminates. This resistance is particularly relevant in the present case, where the applied load consists of moment acting about the *y*-axis, on the left and right edges of the laminate. Such moments induce bending that is highly resisted by the tensile forces generated within the laminate. As the unidirectional fibers are oriented in the direction that effectively encounter this tensile strength. Regarding the anti-symmetric laminates, the extensional matrix is the same for both symmetric and anti-symmetric. Also, the bending matrix is the same except for elements D_{16} and D_{26}. However, the effect of these elements is small compared to the coupling effect represented by the coupling matrix, which directs portion of the energy to induce shear, thus hindering the bending effect.

3.2. Cases Under Pressure Loading. Laminates under pressure loading exhibited the same behavior as laminates under moment loading. Further, the observations made on cases under moment loading are extended for those under pressure loading.

For all cases, the displacement pattern is consistent for all laminates, and the response is composed of a single frequency as indicated by Figures 12, 13, and 14 and Figures 15, 16, and 17, respectively. Table 6 provides data about the quasi-static and maximum amplitudes of laminates under pressure loading, where the consistency of the results between cases under moment loading and under pressure loading is evident. This indicates that a different load did not affect the qualitative pattern or frequency characteristics of the response.

3.3. Frequency Characteristics of the Response. To determine the effect of the constituent materials on the response characteristics, a comparison is made between the natural frequency of the materials and the response frequency, which is provided by Figures 9, 10, and 11 for cases under moment loading, and Figures 15, 16, and 17 for cases under pressure loading. The constituent materials, fiber and epoxy, are each studied using three different models. The first model considers the material as a single lamina, the second model considers the material as a single-material laminate, but taking into account the effect of the other material on the reference material. This is done by utilizing the method of transformed sections. The last model considers the material as a single-material laminate. The modal results obtained analytically based on the following equations [31]:

$$\omega_{mn}^2 = \frac{\pi^4}{\rho b^4}\left[D_{11}m^4 + 2(D_{12} + 2D_{66})m^2n^2 + D_{22}n^2\right] \quad (1)$$

The natural frequency for the constituent materials is provided in Tables 7 and 8.

Consider Figure 18, which represents the undamped response of the unidirectional laminate under pressure load with thickness to length ratio of 0.0375. Since the response is amplitude modulated, it is affected by two waveforms,

3962, 2026, 1, Downloaded from https://onlinelibrary.wiley.com/doi/10.1155/je/9725460 by Turkey Cochrane Evidence Aid, Wiley Online Library on [01/10/2026]. See the Terms and Conditions (https://onlinelibrary.wiley.com/terms-and-conditions) on Wiley Online Library for rules of use; OA articles are governed by the applicable Creative Commons License

TABLE 9: Modal data of the laminates.

Model type	Thickness/ length	Carrier frequency (Hz)	Modulating frequency (Hz)
Unidirectional	0.0125	501	18
Cross-ply	0.0125	501	16
Symmetric-30	0.0125	501	20
Symmetric-45	0.0125	501	18
Anti-symm-30	0.0125	501	20
Anti-symm-45	0.0125	501	18
Unidirectional	0.025	501	10
Cross-ply	0.025	501	10
Symmetric-30	0.025	501	12
Symmetric-45	0.025	501	14
Anti-symm-30	0.025	501	12
Anti-symm-45	0.025	501	14
Unidirectional	0.0375	501	10
Cross-ply	0.0375	501	10
Symmetric-30	0.0375	501	10
Symmetric-45	0.0375	501	12
Anti-symm-30	0.0375	501	10
Anti-symm-45	0.0375	501	12

modulating wave and carrier wave, where the carrier frequency represents the core wave of the response, and the modulating wave will modulate the amplitude of the core wave. The frequency of the carrier wave is the same as the response frequency, around 500 Hz, as indicated by the Fourier transform figures. And the modulating frequency can be determined by subtracting the carrier frequency (501 Hz) from the upper band (511 Hz), which is 10 Hz. For most cases with thickness to length ratio of 0.025 and 0.0375, the modulating frequency is 10 Hz, as shown in Table 9. The ratio of the carrier frequency to the modulating frequency is 50.1, closely mirroring the ratio between the elasticity modulus of the fiber and that of the matrix. This similarity highlights the consistent influence of the constituent materials on the frequency modulation ratio. However, the modulating frequency for laminates with thickness to length ratio of 0.0125 is higher than other cases. This result indicates a faster oscillating response, suggesting that the laminate is more sensitive to the applied forces. The increased sensitivity is likely due to the laminate's thinness, which reduces stiffness and weakens its structural response.

Referring to Tables 7, 8, and 9, even though the values does not match, but it does give an indication that the modulating frequency is due to the epoxy. Whereas, per Table 9, the modulating frequency ranges from 10 to 20 Hz, and from Tables 7 and 8, it ranges from 4 to 22 Hz. Further, the carrier frequency originates from the fiber.

The amplitude of the carrier frequency in the Fourier transform for a given thickness is not significantly influenced by the stacking sequence. As shown by Figure 15 for instance, the carrier frequency amplitude is around (0.25e −5) for all laminates, with only minor variations. The carrier frequency corresponds to the natural frequency of the plate, which is primarily governed by its the stiffness and mass. Although changes in the stacking sequence affect the stiffness, these variations result in only slight differences in the carrier frequency amplitude.

However, the stacking sequence has a substantial impact on the modulation amplitude. For instance, in Figure 15, the unidirectional laminate exhibits a higher carrier frequency amplitude 0.2545e−5, compared to the cross-ply laminate 0.225e−5. On the other hand, the modulation amplitude in the unidirectional laminate is higher, resulting in a higher deformation than the cross-ply laminate. The same qualitative analysis can be extended to the symmetric antisymmetric laminates, and for all thicknesses, reinforcing the observations mentioned in section 3.1 and 3.2.

4. Conclusion

In conclusion, this investigation into the dynamic response of laminated composite plates under sudden loading revealed that:

1. The stacking sequence governs the modulation characteristics of the response, primarily affecting the amplitude of the modulating wave without altering the fundamental carrier frequencies, which are determined by fiber stiffness.
2. The thickness-to-length ratio directly controls the laminate's global stiffness, which in turn dictates the amplitude of the carrier frequency and the quasi-static component of the response.
3. The type of loading had a negligible influence on both the amplitude and frequency characteristics of the dynamic response.
4. The dynamic response is characterized by a carrier frequency, originating from the fiber-dominated stiffness, which is amplitude-modulated by a wave associated with the epoxy matrix.
5. In very thin laminates, the low global stiffness leads to an unexpected increase in the modulating frequency, indicating a high sensitivity to external loads.
6. The presence of initial curvature did not suppress the modulation phenomenon nor alter its frequency content.

Data Availability Statement

The data utilized from the literature and the data generated by ANSYS software that are used to support the findings of this study are included within the article.

3962, 2026, 1, Downloaded from https://onlinelibrary.wiley.com/doi/10.1155/je/9725460 by Turkey Cochrane Evidence Aid, Wiley Online Library on [01/10/2026]. See the Terms and Conditions (https://onlinelibrary.wiley.com/terms-and-conditions) on Wiley Online Library for rules of use; OA articles are governed by the applicable Creative Commons License

Conflicts of Interest

The authors declare no conflicts of interest.

Funding

No funding was received for this manuscript.

Acknowledgments

No AI software has been used to prepare the manuscript; however, DeepSeek AI was used solely for grammar and spelling checks.

References

[1] J. N. Reddy, "Equations of Anisotropic Elasticity, Virtual Work Principles, and Variational Methods," in *Mechanics of Laminated Composite Plates and Shells, Theory and Analysis* (CRC Press, 2nd edition, 2003), https://books.google.jo/books?hl=en%26lr=%26id=eeUr_AJiGRcC%26oi=fnd%26pg=PR19%26dq=J.+N.+Reddy+mechanics+of+Laminated+Composite+Plates+and+Shells,+Theory+and+Analysis,+CRC+Press%26ots=CA9xfgkytt%26sig=XSjLsCCmDapROZJzYVlVnHe9h3s%26redir_esc=y#v=onepage%26q=J.%20N.%20Reddy%20mechanics%20of%20Laminated%20Composite%20Plates%20and%20Shells%2C%20Theory%20and%20Analysis%2C%20CRC%20Press%26f=false.

[2] E. Thornton and R. Foster, "Dynamic Response of Rapidly Heated Space Structures," in *33rd Structures, Structural Dynamics and Materials Conference* (American Institute of Aeronautics and Astronautics, 1992), https://doi.org/10.2514/6.1992-2207.

[3] Mallikarjuna and T. Kant, "Dynamics of Laminated Composite Plates With a Higher Order Theory and Finite Element Discretization," *Journal of Sound and Vibration* 126, no. 3 (1988): 463–475, https://doi.org/10.1016/0022-460X(88)90224-6.

[4] T. Kant and Mallikarjuna, "Transient Dynamics of Composite Sandwich Plates Using 4-, 8-, 9-Noded Isoparametric Quadrilateral Elements," *Finite Elements in Analysis and Design* 5, no. 4 (1989): 307–318, https://doi.org/10.1016/0168-874X(89)90010-3.

[5] T. Kant, C. P. Arora, and J. H. Varaiya, "Finite Element Transient Analysis of Composite and Sandwich Plates Based on a Refined Theory and a Mode Superposition Method," *Composite Structures* 22, no. 2 (1992): 109–120, https://doi.org/10.1016/0263-8223(92)90071-J.

[6] A. Carvalho and C. G. Soares, "Dynamic Response of Rectangular Plates of Composite Materials Subjected to Impact Loads," *Composite Structures* 34, no. 1 (1996): 55–63, https://doi.org/10.1016/0263-8223(95)00131-X.

[7] J. Chen, D. J. Dawe, and S. Wang, "Nonlinear Transient Analysis of Rectangular Composite Laminated Plates," *Composite Structures* 49, no. 2 (2000): 129–139, https://doi.org/10.1016/S0263-8223(99)00108-7.

[8] Y. Y. Wang, K. Y. Lam, and G. R. Liu, "A Strip Element Method for the Transient Analysis of Symmetric Laminated Plates," *International Journal of Solids and Structures* 38, no. 2 (2001): 241–259, https://doi.org/10.1016/S0020-7683(00)00035-4.

[9] M. Ganapathi, B. P. Patel, and D. P. Makhecha, "Nonlinear Dynamic Analysis of Thick Composite/Sandwich Laminates Using an Accurate Higher-Order Theory," *Composites. Part B, Engineering* 35, no. 4 (2004): 345–355, https://doi.org/10.1016/S1359-8368(02)00075-6.

[10] M. Amabili and S. Farhadi, "Shear Deformable Versus Classical Theories for Nonlinear Vibrations of Rectangular Isotropic and Laminated Composite Plates," *Journal of Sound and Vibration* 320, no. 3 (2009): 649–667, https://doi.org/10.1016/j.jsv.2008.08.006.

[11] M. Amabili, K. Karazis, and K. Khorshidi, "Nonlinear Vibrations of Rectangular Laminated Composite Plates With Different Boundary Conditions," *International Journal of Structural Stability and Dynamics* 11, no. 4 (2011): 673–695, https://doi.org/10.1142/S0219455411004294.

[12] Z. Kazancı and Z. Mecitoğlu, "Nonlinear Dynamic Behavior of Simply Supported Laminated Composite Plates Subjected to Blast Load," *Journal of Sound and Vibration* 317, no. 3–5 (2008): 883–897, https://doi.org/10.1016/j.jsv.2008.03.033.

[13] Z. Kazanci, "Nonlinear Transient Response of a Laminated Composite Plate Under Time-Dependent Pulses," in *Proceedings of the 2009 4th International Conference on Recent Advances in Space Technologies* (IEEE, 2009), 125–130, https://doi.org/10.1109/RAST.2009.5158181.

[14] S. Baştürk, H. Uyanık, and Z. Kazancı, "Nonlinear Damped Vibrations of a Hybrid Laminated Composite Plate Subjected to Blast Load," *Procedia Engineering* 88 (2014): 18–25, https://doi.org/10.1016/j.proeng.2014.11.121.

[15] R. P. Khandelwal, A. Chakrabarti, and P. Bhargava, "Vibration Response of Laminated Composite Plate Having Weakly Bonded Layers," *Applied Mathematical Modelling* 39, no. 17 (2015): 5073–5090, https://doi.org/10.1016/j.apm.2015.04.008.

[16] Z. Kazancı, "A Review on the Response of Blast Loaded Laminated Composite Plates," *Progress in Aerospace Science* 81 (2016): 49–59, https://doi.org/10.1016/j.paerosci.2015.12.004.

[17] D. Shao, F. Hu, Q. Wang, F. Pang, and S. Hu, "Transient Response Analysis of Cross-Ply Composite Laminated Rectangular Plates With General Boundary Restraints by the Method of Reverberation Ray Matrix," *Composite Structures* 152 (2016): 168–182, https://doi.org/10.1016/j.compstruct.2016.05.035.

[18] D. Balkan, Ö. Demir, and A. Arıkoğlu, "Dynamic Analysis of a Stiffened Composite Plate Under Blast Load: A New Model and Experimental Validation," *International Journal of Impact Engineering* 143 (2020): 103591, https://doi.org/10.1016/j.ijimpeng.2020.103591.

[19] L. Praticò, J. Galos, E. Cestino, G. Frulla, and P. Marzocca, "Experimental and Numerical Vibration Analysis of Plates With Curvilinear Sub-Stiffeners," *Engineering Structures* 209 (2020): 109956, https://doi.org/10.1016/j.engstruct.2019.109956.

[20] S. N. Akour and J. F. Nayfeh, "Thermally Induced Displacement in Simply-Supported Laminates," *International Journal of Structural Stability and Dynamics* 5, no. 1 (2005): 55–73, https://doi.org/10.1142/S0219455405001489.

[21] S. Akour, "Dynamic Response of Composite Plate Subjected to Sudden Heat Flux," *Modern Applied Science* 11, no. 12 (2017): 36, https://doi.org/10.5539/mas.v11n12p36.

[22] S. N. Akour, "Response of Balanced Laminate Subjected to Abrupt Heat Flux: A New Perspective," *Scientific World Journal* 2022 (2022): 9491939, https://doi.org/10.1155/2022/9491939.

3962, 2026, 1, Downloaded from https://onlinelibrary.wiley.com/doi/10.1155/je/9725460 by Turkey Cochrane Evidence Aid, Wiley Online Library on [01/10/2026]. See the Terms and Conditions (https://onlinelibrary.wiley.com/terms-and-conditions) on Wiley Online Library for rules of use; OA articles are governed by the applicable Creative Commons License

[23] R. Barbaz-Isfahani, H. Dadras, S. Saber-Samandari, A. Taherzadeh-Fard, and G. Liaghat, "A Comprehensive Investigation of the Low-Velocity Impact Response of Enhanced GFRP Composites With Single and Hybrid Loading of Various Types of Nanoparticles," *Heliyon* 9, no. 5 (2023): e15930, https://doi.org/10.1016/j.heliyon.2023.e15930.

[24] K. Xie, Y. Wang, H. Chen, J. Li, and Y. Wang, "Nonlinear Dynamic Response of a Sandwich Plate With Negative Poisson's Ratio Honeycomb-Core Layer Under Low-Velocity Collision Impact," *Computers and Structures* 304 (2024): 107507, https://doi.org/10.1016/j.compstruc.2024.107507.

[25] O. Das, H. Ozturk, C. Gonenli, O. Das, H. Ozturk, and C. Gonenli, "Free vibration and Buckling Analyses of Curved Plate Frames Using Finite Element Method," *Structural Engineering and Mechanics* 86, no. 6 (2023): 765, https://doi.org/10.12989/SEM.2023.86.6.765.

[26] O. Das, H. Ozturk, C. Gonenli, O. Das, H. Ozturk, and C. Gonenli, "Finite Element Vibration Analysis of Laminated Composite Parabolic Thick Plate Frames," *Steel & Composite Structures* 35, no. 1 (2020): 43, https://doi.org/10.12989/SCS.2020.35.1.043.

[27] C. Gonenli, H. Ozturk, and O. Das, "Effect of Crack on Free Vibration of a pre-Stressed Curved Plate," *Proceedings of the Institution of Mechanical Engineers, Part C: Journal of Mechanical Engineering Science* 236, no. 2 (2022): 811–825, https://doi.org/10.1177/0954406221994869.

[28] "PYROFIL TM HR40 High Modulus Carbon Fiber Product Data Sheet," Accessed November 8, 2025, https://fileserver.mates.it/Prodotti/1_Rinforzi/TDS/Carbonio/Fibre/Pyrofil%2520HR40%252012K.pdf.

[29] "Resin Epoxy (Araldite LY1564)," Accessed November 8, 2025, https://www.swiss-composite.ch/pdf/t-Araldite-LY1564-Aradur3486-3487-e.pdf.

[30] S. Swaddiwudhipong and Z. S. Liu, "Response of Laminated Composite Plates and Shells," *Composite Structures* 37, no. 1 (1997): 21–32, https://doi.org/10.1016/S0263-8223(97)00051-2.

[31] R. F. Gibson, *Principles of Composite Material Mechanics* (CRC Press, 2007).

3962, 2026, 1, Downloaded from https://onlinelibrary.wiley.com/doi/10.1155/je/9725460 by Turkey Cochrane Evidence Aid, Wiley Online Library on [01/10/2026]. See the Terms and Conditions (https://onlinelibrary.wiley.com/terms-and-conditions) on Wiley Online Library for rules of use; OA articles are governed by the applicable Creative Commons License